Hindawi
Mathematical Problems in Engineering
Volume 2017, Article ID 9402964, 20 pages
https://doi.org/10.1155/2017/9402964

Research Article

MHD Flow of Micropolar Fluid over an Oscillating Vertical Plate Embedded in Porous Media with Constant Temperature and Concentration

Nadeem Ahmad Sheikh,[1] Farhad Ali,[1] Ilyas Khan,[2] Muhammad Saqib,[1] and Arshad Khan[3]

[1]*Department of Mathematics, City University of Science and Information Technology, Peshawar 25000, Pakistan*
[2]*Basic Engineering Sciences Department, College of Engineering, Majmaah University, Al Majmaah 11952, Saudi Arabia*
[3]*Department of Computer Science, Sarhad University of Science and Information Technology, Peshawar 25000, Pakistan*

Correspondence should be addressed to Farhad Ali; farhadaliecomaths@yahoo.com

Received 5 September 2016; Accepted 19 December 2016; Published 7 February 2017

Academic Editor: Mohamed Abd El Aziz

The present analysis represents the MHD flow of micropolar fluid past an oscillating infinite vertical plate embedded in porous media. At the plate, free convections are caused due to the differences in temperature and concentration. Therefore, the combined effect of radiative heat and mass transfer is taken into account. Partial differential equations are used in the mathematical formulation of a micropolar fluid. The system of dimensional governing equations is reduced to dimensionless form by means of dimensional analysis. The Laplace transform technique is applied to obtain the exact solutions for velocity, temperature, and concentration. In order to highlight the flow behavior, numerical computation and graphical illustration are carried out. Furthermore, the corresponding skin friction and wall couple stress are calculated.

1. Introduction

The effect of MHD can be observed in several natural and artificial flows. MHD is the study of the interaction of conducting fluids with electromagnetic phenomena. Electrically conducting fluids in the presence of a magnetic field are of importance in many areas of technology and engineering such as MHD flow meters, MHD power generation, and MHD pumps. It is generally accepted that various astronomical bodies (e.g., Earth, the sun, Jupiter, magnetic stars, and pulsars) acquire fluid interiors and magnetic fields [1]. In the recent past, extensive consideration has been given to applications of MHD and heat transfer such as MHD generators, metallurgical processing, and geothermal energy extraction. The MHD flow with combined effects of heat and mass transfer has wide applications in science and technology, for example, quasi-solid bodies such as earth and in buoyancy induced flows in the atmosphere [2]. Prakash et al. [3] analyzed the effects of thermal diffusion and chemical reaction on MHD boundary layer flow of electrically conducting dusty fluid between two vertical heated plates. Shahid [4] obtained the exact solutions for MHD free convection flow of generalized viscous fluid over an oscillating plate. Raju and Sandeep [5] investigated the MHD flow of non-Newtonian fluid over a rotating cone with cross-diffusion. Therefore, the MHD flow with combined effect of heat and mass transfer has been a subject of concern of several researchers including [6–13].

The flow of non-Newtonian fluids through porous medium has been of considerable interest in the last few decades. This interest is because several practical applications can be modeled as transport phenomena in a porous medium. These flows emerge at a large scale in a variety of industrial applications as well as in natural situations, that is, cooling of electronic components, casting and welding of manufacturing processes, food processing, packed-bed reactors, storage of nuclear waste material, oil recovery processes, thermal insulation engineering, pollutant dispersion in aquifers, ground water flows, geothermal extraction, fibrous insulation, industrial and agricultural water distribution, soil pollution, liquid metal flow through generic structures in alloy casting, and the dispersion of chemical

contaminants in various processes in the chemical industry [14]. This area of research is of fundamental interest in view of the above applications, thereby generating the need for full understanding of transport processes through a porous medium. Abo-Eldahab and Ghonaim [15] obtained the numerical solutions by applying an efficient numerical technique based on the shooting method for convective flow of micropolar fluid in a porous medium. Kim [16] presented the analysis for the free convection with mass transfer flow of a micropolar fluid through a porous medium bounded by a semi-infinite vertical permeable plate in the presence of a transverse magnetic field. Modather et al. [17] analyzed the convective flow of a micropolar fluid over an infinite moving porous plate in a saturated porous medium in the presence of a transverse magnetic field and obtained the analytical solutions. Many researchers have considered the flow through a porous medium in their studies [18–25].

Originally, the theory of a micropolar fluid was presented by Eringen in 1966 [26]. In the recent decades, the study of micropolar fluid is a popular field of research. In micropolar fluid, the randomly oriented particles are suspended in a viscous medium that can experience a rotation that can affect the hydrodynamics of the flow which makes it a distinctly non-Newtonian fluid. An excellent model for analyzing various complex fluids such as blood, polymeric fluids, and colloidal fluids was proposed in Eringen's theory [26]. The study of free convection MHD flow of a micropolar fluid over an oscillating infinite vertical plate saturated porous medium has important applications in geophysics and engineering and technology. These applications included the boundary layer control in the field of aerodynamics, MHD generators, extraction of geothermal resources, petroleum resource extraction, and nuclear reactors [27]. Nazar et al. [28] used the Keller-Box method to obtain the numerical solutions for a steady flow of micropolar fluid over a stretching sheet. Nadeem et al. [29] considered the unsteady MHD flow of micropolar fluid near a forward stagnation point of two-dimensional plane surface. They solved the governing equations using homotopy analysis method. Many scholars studied micropolar fluids in various geometries applying different mathematical tools [30–36]. Recently, Khalid et al. [37] reported the exact solutions via Laplace transform technique for the analysis of combined effects of heat and mass transfer of micropolar fluid over an oscillating plate. Motivated by the above investigations, the present analysis is focused on the study of MHD flow of micropolar fluid over an oscillating vertical plate embedded in a porous medium in the presence of thermal radiation. Exact solutions are obtained using the Laplace transform technique.

2. Mathematical Formulation

The unsteady flow of an incompressible electrically conducting micropolar fluid in a porous medium is considered. Initially both the fluid and infinite vertical plate are in the state of rest with uniform temperature T_∞ and concentration C_∞. At $t = 0^+$ the plate starts oscillations in its own plane with constant frequency ω and amplitude u_0. The temperature and concentration of the plate are raised to T_w and C_w linearly

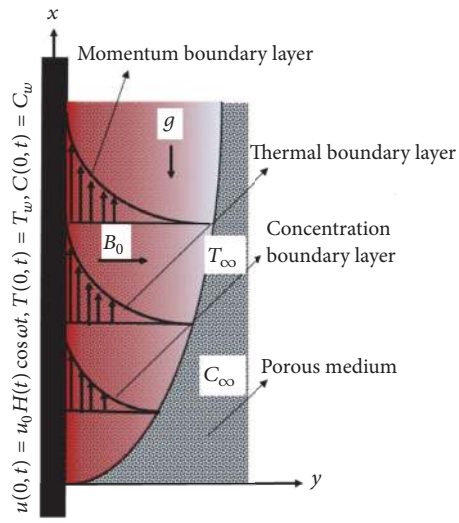

Figure 1: Physical sketch.

with t. The fluid starts motion in x-direction along the plate and y-axis is taken normal to the plate. Magnetic field of uniform strength B_0 is applied transverse to the plate and induced magnetic field is not taken into consideration due to enough small Reynold number. Physical geometry of the problem is presented in Figure 1.

By using the Boussinesq approximation, the governing equations of the problem under consideration are given as follows:

$$\begin{aligned}
\rho\frac{\partial u}{\partial t} &= (\mu+\alpha)\frac{\partial^2 u}{\partial y^2} + \alpha\frac{\partial N}{\partial y} - \sigma B_0^2 u - \frac{\phi_1\mu}{k}u \\
&\quad + \rho g\beta_T (T - T_\infty) + \rho g\beta_C (C - C_\infty), \\
\rho j\frac{\partial N}{\partial y} &= \gamma\frac{\partial^2 N}{\partial y^2}, \\
\rho c_p\frac{\partial T}{\partial t} &= k_1\frac{\partial^2 T}{\partial y^2} - \frac{\partial q_r}{\partial y}, \\
\frac{\partial C}{\partial t} &= D\frac{\partial^2 C}{\partial y^2},
\end{aligned} \tag{1}$$

subject to the following initial and boundary conditions:

$$\begin{aligned}
u(y,0) &= 0, \\
N(y,0) &= 0, \\
T(y,0) &= T_\infty, \\
C(y,0) &= C_\infty, \\
u(0,t) &= u_0 H(t)\cos\omega t, \\
N(0,t) &= -n\frac{\partial u(0,t)}{\partial y},
\end{aligned}$$

$$
\begin{aligned}
T(0,t) &= T_w,\\
C(0,t) &= C_w,\\
u(\infty,t) &= 0,\\
N(\infty,t) &= 0,\\
T(\infty,t) &= T_\infty,\\
C(\infty,t) &= C_\infty.
\end{aligned}
\tag{2}
$$

Here,

$$
q_r = -\frac{4\sigma_1}{3k_2}\frac{\partial T^4}{\partial y}, \tag{3}
$$

where σ_1 is the Stefan-Boltzmann constant and k_2 is the mean absorption coefficient. Considering small temperature difference between fluid temperature T and free stream temperature T_∞, T^4 is expanded in Taylor series about the free stream temperature T_∞. Neglecting second- and higher-order terms in $(T - T_\infty)$, we get

$$
T^4 = 4TT_\infty^3 - 3T_\infty^4. \tag{4}
$$

In the above equations, ν is the kinematic viscosity, α is the vortex viscosity, ρ is the fluid density, μ is the dynamic viscosity, ϕ_1 $(0 < \phi_1 < 1)$ and $k > 0$ are the porosity and permeability of the porous medium, respectively, σ is the electrical conductivity, g is the gravitational acceleration, β_T is the coefficient of thermal expansion, and β_C is the coefficient of concentration expansion. j is the microinertia per unit mass and γ is the spin gradient. T is the fluid temperature, c_p is the specific heat capacity, k_1 is the thermal conductivity, q_r is radioactive flux, C is the species concentration, D is the mass diffusivity, ω is the frequency of the velocity of the wall, and $H(t)$ is the unit step function. Three distinct values of $0 \le n \le 1$, when $n = 0$, which show $N = 0$ at the wall represent concentrated particle flows in which the microelements near to the wall are unable to rotate; this situation is also called strong concentration of microelements. When $n = 1/2$, it indicates the vanishing of antisymmetric part of the stress tensor and describes weak concentration of microelements. The case when $n = 1$ is used for the modelling of turbulent boundary layer flows [37].

We introduce the dimensionless variables,

$$
\begin{aligned}
\nu &= \frac{u}{u_0},\\
\xi &= \frac{u_0}{\nu}y,\\
\tau &= \frac{u_0^2}{\nu}t,\\
\Omega &= \frac{\nu N}{u_0^2},\\
\theta &= \frac{T - T_\infty}{T_w - T_\infty},\\
\Phi &= \frac{C - C_\infty}{C_w - C_\infty},
\end{aligned}
\tag{5}
$$

in (1)-(2), yielding

$$
\begin{aligned}
\frac{\partial \nu}{\partial \tau} &= (1+\beta)\frac{\partial^2 \nu}{\partial \xi^2} + \beta\frac{\partial \Omega}{\partial \xi} - K_{\text{eff}}\nu + \text{Gr}\theta\\
&\quad + \text{Gm}\Phi,
\end{aligned}
\tag{6}
$$

$$
\frac{\partial \Omega}{\partial \tau} = \frac{1}{\eta}\frac{\partial^2 \Omega}{\partial \xi^2}, \tag{7}
$$

$$
\frac{\partial \theta}{\partial \tau} = \frac{1}{\text{Pr}_{\text{eff}}}\frac{\partial^2 \theta}{\partial \xi^2}, \tag{8}
$$

$$
\text{Sc}\frac{\partial \Phi}{\partial \tau} = \frac{\partial^2 \Phi}{\partial \xi^2}, \tag{9}
$$

$$
\begin{aligned}
\nu(\xi,0) &= 0,\\
\Omega(\xi,0) &= 0,\\
\theta(\xi,0) &= 0,\\
\Phi(\xi,0) &= 0,\\
\nu(0,\tau) &= H(\tau)\cos\omega\tau,\\
\Omega(0,\tau) &= -n\frac{\partial \nu(0,\tau)}{\partial \xi},\\
\theta(0,\tau) &= 1,\\
\Phi(0,\tau) &= 1,\\
\nu(\infty,\tau) &= 0,\\
\Omega(\infty,\tau) &= 0,\\
\theta(\infty,\tau) &= 0,\\
\Phi(\infty,\tau) &= 0,
\end{aligned}
\tag{10}
$$

where $\beta = \alpha/\mu$ is the dimensionless micropolar fluid parameter, $\text{Gr} = (\nu g\beta_T/u_0^3)(T_w - T_\infty)$ is the thermal Grashof number, $\text{Gm} = (\nu g\beta_C/u_0^3)(C_w - C_\infty)$ is the mass Grashof number, $1/K = \nu^2\phi_1/ku_0^2$ is the permeability parameter of porous medium, $M = \nu\sigma B_0^2/\rho u_0^2$ is the magnetic parameter, $\eta = \mu j/\gamma$ is the spin gradient, $\text{Pr} = \mu c_p/k_1$ is the Prandtl number, $R = 16\sigma_1 T_\infty^3/3k_1k_2$ is the radiation parameter, $\text{Sc} = \nu/D$ is the Schmidt number, and the other constants in calculi are $K_{\text{eff}} = M + 1/K$ and $\text{Pr}_{\text{eff}} = \text{Pr}/(1+R)$.

3. Solution of the Governing Problem

Applying Laplace transforms to (6)–(9) and using corresponding initial conditions from (10), we get

$$\frac{d^2\overline{v}}{d\xi^2} - \delta\left(q + K_{\text{eff}}\right)\overline{v} = \Omega_0\beta\delta - \frac{\delta \text{Gr}\overline{\theta}}{q} - \frac{\delta \text{Gm}\overline{\Phi}}{q}, \tag{11}$$

$$\frac{d^2\overline{\theta}}{d\xi^2} - \text{Pr}_{\text{eff}}\, q\overline{\theta} = 0, \tag{12}$$

$$\frac{d^2\overline{\Phi}}{d\xi^2} - \text{Sc}q\overline{\Phi} = 0, \tag{13}$$

$$\frac{d^2\overline{\Omega}}{d\xi^2} - \eta q\overline{\Omega} = 0. \tag{14}$$

The transformed boundary conditions are

$$\begin{aligned}
\overline{v}(0,q) &= \frac{q}{q^2+\omega^2},\\
\overline{\theta}(0,q) &= \frac{1}{q},\\
\overline{\Phi}(0,q) &= \frac{1}{q},\\
\overline{\Omega}(0,q) &= -n\frac{\partial\overline{v}(0,q)}{\partial\xi} = \Omega_0,\\
\overline{v}(\infty,q) &= 0,\\
\overline{\theta}(\infty,q) &= 0,\\
\overline{\Phi}(\infty,q) &= 0,\\
\overline{\Omega}(\infty,q) &= 0.
\end{aligned} \tag{15}$$

With exact solutions of (12) and (13), taking corresponding boundary conditions from (15) into account, we arrive at

$$\begin{aligned}
\overline{\theta}(\xi,q) &= \frac{1}{q}e^{-\xi\sqrt{\text{Pr}_{\text{eff}}q}},\\
\overline{\Phi}(\xi,q) &= \frac{1}{q}e^{-\xi\sqrt{\text{Sc}q}}.
\end{aligned} \tag{16}$$

Inverting the Laplace transform of (16), we get

$$\begin{aligned}
\theta(\xi,\tau) &= \text{erf}\, c\left(\frac{\xi\sqrt{\text{Pr}_{\text{eff}}}}{2\sqrt{\tau}}\right),\\
\Phi(\xi,\tau) &= \text{erf}\, c\left(\frac{\xi\sqrt{\text{Sc}}}{2\sqrt{\tau}}\right).
\end{aligned} \tag{17}$$

The solution of (11) and (14) with corresponding boundary conditions from (15) and in view of (16) is given by

$$\begin{aligned}
\overline{v}(\xi,q) &= \overline{v}_1(\xi,q) + \overline{v}_2(\xi,q) + \overline{v}_3(\xi,q) - \overline{v}_4(\xi,q)\\
&\quad + \overline{v}_5(\xi,q),\\
\overline{\Omega}(\xi,q) &= \overline{\Omega}_1(\xi,q) + \overline{\Omega}_2(\xi,q),
\end{aligned} \tag{18}$$

where

$$\begin{aligned}
\overline{v}_1(\xi,q) &= A_0\overline{f}\left(\xi\sqrt{\delta},q,-i\omega,K_{\text{eff}}\right)\\
&\quad + A_1\overline{f}\left(\xi\sqrt{\delta},q,i\omega,K_{\text{eff}}\right) - A_2\overline{f}\left(\xi\sqrt{\delta},q,0,K_{\text{eff}}\right)\\
&\quad + A_3\overline{f}\left(\xi\sqrt{\delta},q,a_{11},K_{\text{eff}}\right) + A_4\overline{f}\left(\xi\sqrt{\delta},q,a_{12},K_{\text{eff}}\right)\\
&\quad - A_5\overline{f}\left(\xi\sqrt{\delta},q,-\delta_1,K_{\text{eff}}\right) - A_6\overline{f}\left(\xi\sqrt{\delta},q,\right.\\
&\quad \left.-\delta_2,K_{\text{eff}}\right) - A_7\overline{f}\left(\xi\sqrt{\delta},q,\delta_3,K_{\text{eff}}\right),\\
\overline{v}_2(\xi,q) &= A_7\overline{f}(\xi\sqrt{\eta},q,\delta_3,0) + A_8\overline{f}(\xi\sqrt{\eta},q,a_{11},0)\\
&\quad + A_9\overline{f}(\xi\sqrt{\eta},q,a_{12},0) + A_5\overline{f}(\xi\sqrt{\eta},q,-\delta_1,0)\\
&\quad + A_6\overline{f}(\xi\sqrt{\eta},q,-\delta_2,0) + A_{10}\overline{f}(\xi\sqrt{\eta},q,i\omega,0)\\
&\quad + A_{11}\overline{f}(\xi\sqrt{\eta},q,-i\omega,0),\\
\nu_3(\xi,\tau) &= \lambda_0 f\left(\xi\sqrt{\text{Pr}_{\text{eff}}},\tau,0,0\right)\\
&\quad - \lambda_0 f\left(\xi\sqrt{\text{Pr}_{\text{eff}}},\tau,a_{11},0\right) + \lambda_1 f\left(\xi\sqrt{\text{Sc}},\tau,0,0\right)\\
&\quad - \lambda_1 f\left(\xi\sqrt{\text{Sc}},\tau,a_{12},0\right),\\
\overline{v}_4(\xi,q) &= \sqrt{q}\left[A_{12}\overline{g}\left(\xi\sqrt{\delta},q,0,K_{\text{eff}}\right)\right.\\
&\quad + A_{13}\overline{g}\left(\xi\sqrt{\delta},q,\delta_3,K_{\text{eff}}\right)\\
&\quad + A_{14}\overline{g}\left(\xi\sqrt{\delta},q,a_{11},K_{\text{eff}}\right)\\
&\quad + A_{15}\overline{g}\left(\xi\sqrt{\delta},q,a_{12},K_{\text{eff}}\right)\\
&\quad + A_{16}\overline{g}\left(\xi\sqrt{\delta},q,-\delta_1,K_{\text{eff}}\right)\\
&\quad - A_{17}\overline{g}\left(\xi\sqrt{\delta},q,-\delta_2,K_{\text{eff}}\right)\\
&\quad + A_{18}\overline{g}\left(\xi\sqrt{\delta},q,i\omega,K_{\text{eff}}\right)\\
&\quad \left. - A_{19}\overline{g}\left(\xi\sqrt{\delta},q,-i\omega,K_{\text{eff}}\right)\right],\\
\overline{v}_5(\xi,q) &= \sqrt{q+K_{\text{eff}}}\left[A_{12}\overline{g}(\xi\sqrt{\eta},q,0,0)\right.\\
&\quad + A_{13}\overline{g}(\xi\sqrt{\eta},q,\delta_3,0) + A_{14}\overline{g}(\xi\sqrt{\eta},q,a_{11},0)\\
&\quad + A_{15}\overline{g}(\xi\sqrt{\eta},q,a_{12},0) + A_{16}\overline{g}(\xi\sqrt{\eta},q,-\delta_1,0)\\
&\quad - A_{17}\overline{g}(\xi\sqrt{\eta},q,-\delta_2,0) + A_{18}\overline{g}(\xi\sqrt{\eta},q,i\omega,0)\\
&\quad \left. - A_{19}\overline{g}(\xi\sqrt{\eta},q,-i\omega,0)\right],\\
\overline{\Omega}_1(\xi,q) &= n\sqrt{\delta}\sqrt{q+K_{\text{eff}}}\left[L_1\overline{f}(\xi\sqrt{\eta},q,0,0)\right.\\
&\quad + L_2\overline{f}(\xi\sqrt{\eta},q,a_{11},0) + L_3\overline{f}(\xi\sqrt{\eta},q,a_{12},0)\\
&\quad + L_4\overline{f}(\xi\sqrt{\eta},q,-\delta_1,0) + L_5\overline{f}(\xi\sqrt{\eta},q,-\delta_2,0)\\
&\quad \left. + L_6\overline{f}(\xi\sqrt{\eta},q,i\omega,0) + L_7\overline{f}(\xi\sqrt{\eta},q,-i\omega,0)\right],
\end{aligned}$$

$$\begin{aligned}
\overline{\Omega}_2(\xi,q) &= n\left[L_8\overline{g}(\xi\sqrt{\eta},q,0,0)\right.\\
&\quad + L_9\overline{g}(\xi\sqrt{\eta},q,a_{11},0) + L_{10}\overline{g}(\xi\sqrt{\eta},q,a_{12},0)\\
&\quad + L_{11}\overline{g}(\xi\sqrt{\eta},q,-\delta_1,0) + L_{12}\overline{g}(\xi\sqrt{\eta},q,-\delta_2,0)\\
&\quad \left. + L_{13}\overline{g}(\xi\sqrt{\eta},q,i\omega,0) + L_{14}\overline{g}(\xi\sqrt{\eta},q,\delta_3,0)\right],\\
\overline{f}(\zeta,q,\lambda,b) &= \frac{1}{q-\lambda}\exp\left(-\zeta\sqrt{q+b}\right),\\
\overline{g}(\zeta,q,\lambda,b) &= \frac{\sqrt{q+b}}{q-\lambda}\exp\left(-\zeta\sqrt{q+b}\right).
\end{aligned} \tag{19}$$

For A_i, $i = 1,2,\ldots,19$, and L_j, $j = 1,2,\ldots,14$, see Appendix.

The Laplace inverse transforms of (18) are given by

$$\begin{aligned}
v(\xi,\tau) &= v_1(\xi,\tau) + v_2(\xi,\tau) + v_3(\xi,\tau) - v_4(\xi,\tau)\\
&\quad + v_5(\xi,\tau),\\
\Omega(\xi,\tau) &= \Omega_1(\xi,\tau) + \Omega_2(\xi,\tau),
\end{aligned} \tag{20}$$

where

$$\begin{aligned}
v_1(\xi,\tau) &= A_0 f\left(\xi\sqrt{\delta},\tau,-i\omega,K_{\text{eff}}\right)\\
&\quad + A_1 f\left(\xi\sqrt{\delta},\tau,i\omega,K_{\text{eff}}\right) - A_2 f\left(\xi\sqrt{\delta},\tau,0,K_{\text{eff}}\right)\\
&\quad + A_3 f\left(\xi\sqrt{\delta},\tau,a_{11},K_{\text{eff}}\right) + A_4 f\left(\xi\sqrt{\delta},\tau,a_{12},K_{\text{eff}}\right)\\
&\quad - A_5 f\left(\xi\sqrt{\delta},\tau,-\delta_1,K_{\text{eff}}\right) - A_6 f\left(\xi\sqrt{\delta},\tau,\right.\\
&\quad \left. -\delta_2,K_{\text{eff}}\right) - A_7 f\left(\xi\sqrt{\delta},\tau,\delta_3,K_{\text{eff}}\right),\\
v_2(\xi,\tau) &= A_7 f(\xi\sqrt{\eta},\tau,\delta_3,0) + A_8 f(\xi\sqrt{\eta},\tau,a_{11},0)\\
&\quad + A_9 f(\xi\sqrt{\eta},\tau,a_{12},0) + A_5 f(\xi\sqrt{\eta},\tau,-\delta_1,0)\\
&\quad + A_6 f(\xi\sqrt{\eta},\tau,-\delta_2,0) + A_{10} f(\xi\sqrt{\eta},\tau,i\omega,0)\\
&\quad + A_{11} f(\xi\sqrt{\eta},\tau,-i\omega,0),\\
v_3(\xi,\tau) &= \lambda_0 f\left(\xi\sqrt{\text{Pr}_{\text{eff}}},\tau,0,0\right)\\
&\quad - \lambda_0 f\left(\xi\sqrt{\text{Pr}_{\text{eff}}},\tau,a_{11},0\right) + \lambda_1 f\left(\xi\sqrt{\text{Sc}},\tau,0,0\right)\\
&\quad - \lambda_1 f\left(\xi\sqrt{\text{Sc}},\tau,a_{12},0\right),\\
v_4(\xi,\tau) &= -\left(\frac{1}{2\tau\sqrt{\pi\tau}}\right) * \left[A_{12} g\left(\xi\sqrt{\delta},\tau,0,K_{\text{eff}}\right)\right.\\
&\quad + A_{13} g\left(\xi\sqrt{\delta},\tau,\delta_3,K_{\text{eff}}\right)\\
&\quad + A_{14} g\left(\xi\sqrt{\delta},\tau,a_{11},K_{\text{eff}}\right)\\
&\quad + A_{15} g\left(\xi\sqrt{\delta},\tau,a_{12},K_{\text{eff}}\right)\\
&\quad + A_{16} g\left(\xi\sqrt{\delta},\tau,-\delta_1,K_{\text{eff}}\right)\\
&\quad - A_{17} g\left(\xi\sqrt{\delta},\tau,-\delta_2,K_{\text{eff}}\right)\\
&\quad + A_{18} g\left(\xi\sqrt{\delta},\tau,i\omega,K_{\text{eff}}\right)\\
&\quad \left. - A_{19} g\left(\xi\sqrt{\delta},\tau,-i\omega,K_{\text{eff}}\right)\right],\\
v_5(\xi,\tau) &= -\left(\frac{1}{2\tau\sqrt{\pi\tau}} e^{-K_{\text{eff}}\tau}\right) * \left[A_{12} g\left(\xi\sqrt{\delta},\tau,0,0\right)\right.\\
&\quad + A_{13} g\left(\xi\sqrt{\delta},\tau,\delta_3,0\right) + A_{14} g\left(\xi\sqrt{\delta},\tau,a_{11},0\right)\\
&\quad + A_{15} g\left(\xi\sqrt{\delta},\tau,a_{12},0\right) + A_{16} g\left(\xi\sqrt{\delta},\tau,-\delta_1,0\right)\\
&\quad - A_{17} g\left(\xi\sqrt{\delta},\tau,-\delta_2,0\right) + A_{18} g\left(\xi\sqrt{\delta},\tau,i\omega,0\right)\\
&\quad \left. - A_{19} g\left(\xi\sqrt{\delta},\tau,-i\omega,0\right)\right],\\
\Omega_1(\xi,\tau) &= -n\sqrt{\delta}\left(\frac{1}{2\tau\sqrt{\pi\tau}} e^{-K_{\text{eff}}\tau}\right)\\
&\quad * \left[L_1 f(\xi\sqrt{\eta},\tau,0,0) + L_2 f(\xi\sqrt{\eta},\tau,a_{11},0)\right.\\
&\quad + L_3 f(\xi\sqrt{\eta},\tau,a_{12},0) + L_4 f(\xi\sqrt{\eta},\tau,-\delta_1,0)\\
&\quad + L_5 f(\xi\sqrt{\eta},\tau,-\delta_2,0) + L_6 f(\xi\sqrt{\eta},\tau,i\omega,0)\\
&\quad \left. + L_7 f(\xi\sqrt{\eta},\tau,-i\omega,0)\right],\\
\Omega_2(\xi,\tau) &= n\left[L_8 g(\xi\sqrt{\eta},\tau,0,0) + L_9 g(\xi\sqrt{\eta},\tau,a_{11},0)\right.\\
&\quad + L_{10} g(\xi\sqrt{\eta},\tau,a_{12},0) + L_{11} g(\xi\sqrt{\eta},\tau,-\delta_1,0)\\
&\quad + L_{12} g(\xi\sqrt{\eta},\tau,-\delta_2,0) + L_{13} g(\xi\sqrt{\eta},\tau,i\omega,0)\\
&\quad \left. + L_{14} g(\xi\sqrt{\eta},\tau,\delta_3,0)\right],\\
f(\xi,\tau,\lambda,b) &= \frac{\exp(\lambda\tau)}{2}\left[\exp\left(-\xi\sqrt{\lambda+b}\right)\text{erf}\,c\right.\\
&\quad \cdot\left(\frac{\xi}{2\sqrt{\tau}} - \sqrt{(\lambda+b)\tau}\right) + \exp\left(\xi\sqrt{\lambda+b}\right)\text{erf}\,c\\
&\quad \left.\cdot\left(\frac{\xi}{2\sqrt{\tau}} + \sqrt{(\lambda+b)\tau}\right)\right],\\
g(\xi,\tau,\lambda,b) &= (\lambda+b)\frac{\exp(\lambda\tau)}{2\sqrt{\lambda+b}}\left[\exp\left(-\xi\sqrt{\lambda+b}\right)\text{erf}\,c\right.\\
&\quad \cdot\left(\frac{\xi}{2\sqrt{\tau}} - \sqrt{(\lambda+b)\tau}\right) - \exp\left(\xi\sqrt{\lambda+b}\right)\text{erf}\,c\\
&\quad \left.\cdot\left(\frac{\xi}{2\sqrt{\tau}} + \sqrt{(\lambda+b)\tau}\right)\right] + \frac{1}{\sqrt{\pi\tau}}\exp\left(-\frac{\xi^2}{4\tau} - b\tau\right);
\end{aligned} \tag{21}$$

here, $f * g$ shows the convolution product of f and g.

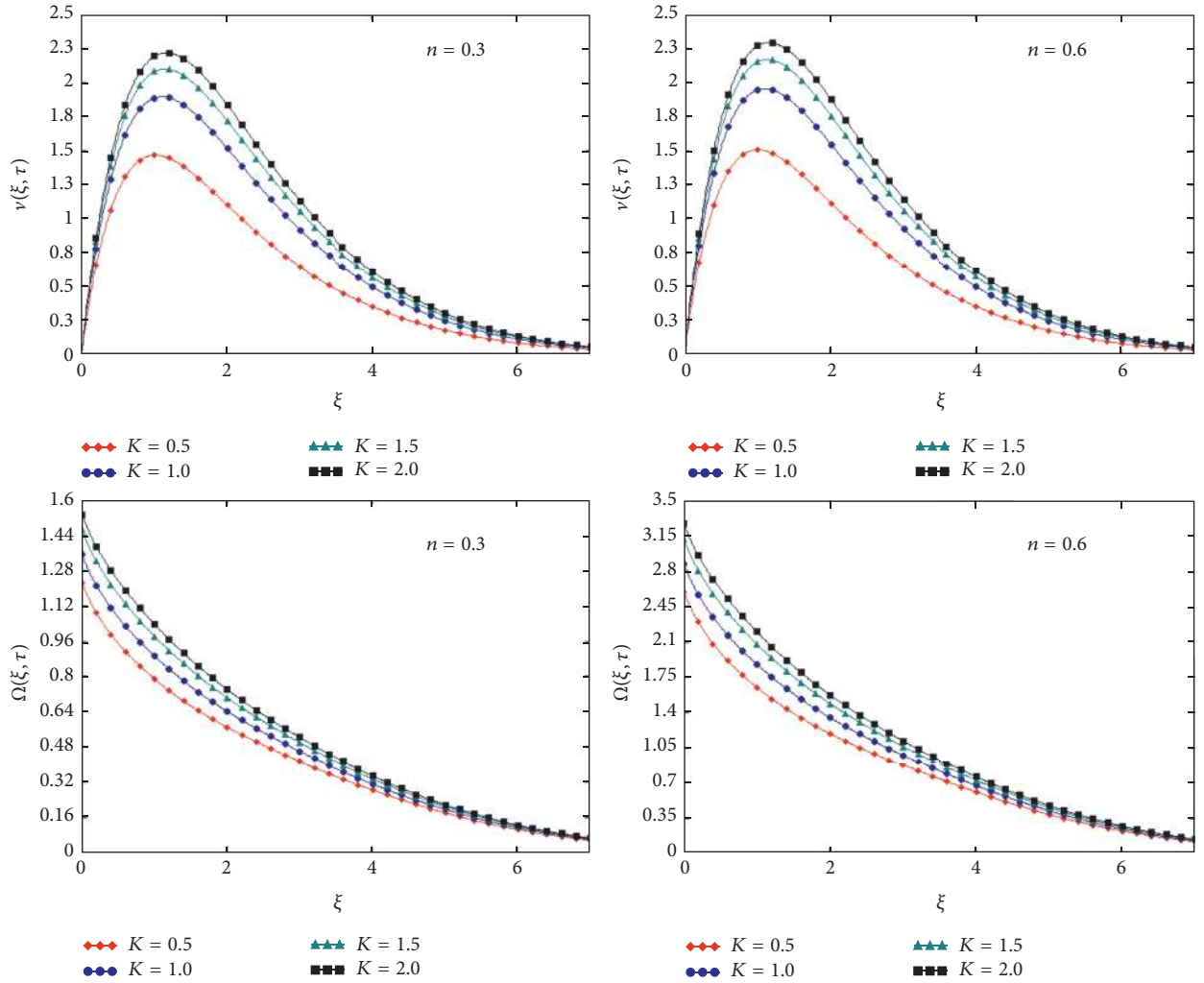

Figure 2: Variation in velocity and microrotation for different value of K and n.

The coefficient of skin friction C_f and coefficient of couple stress C_s are important physical quantities, which in dimensionless form are defined as follows:

$$C_f = 2\{1 + (1-n)\beta\} \left.\frac{\partial v(\xi,\tau)}{\partial \xi}\right|_{\xi=0},$$
$$C_s = \left.\frac{\partial \Omega(\xi,\tau)}{\partial \xi}\right|_{\xi=0}. \quad (22)$$

4. Results and Discussion

Exact solutions are obtained and the results are plotted for various embedded parameters, namely, permeability parameter K, magnetic parameter M, radiation parameter R, Prandtl number Pr, thermal Grashof number Gr, mass Grashof number Gm, spin gradient parameter η, and micropolar fluid parameter β on velocity and microrotation distributions in order to highlight the flow behavior. Skin friction and couple stress coefficient are also calculated numerically and presented in tabular form.

Figures 2–15 are plotted to show the effects of different embedded parameters on velocity and microrotation profiles. From these figures, it is noticed that velocity, as well as the magnitude of microrotation, decreases with increasing magnetic parameter M. Physically, it is true because it gives rise to a resistive force called the Lorentz force. The velocity and microrotation profiles for different values of the permeability parameter K are also displayed. It is obvious from the figures that an increase in K decreases the drag force and causes the velocity and magnitude of microrotation to increase.

Figures 2 and 3 depicted the influence of n on the velocity and microrotation profiles, which relates to the shear stress and microgyration vector. The velocity and magnitude of microrotation show an increasing behavior for greater values of n. It is observed in Figures 4 and 5 that velocity and magnitude of microrotation decrease with increasing R; this can be explained by the fact that radiation diffuses energy and reduces temperature; consequently, the velocity and magnitude of microrotation decrease. Figures 6 and 7 depict the effect of Prandtl number Pr on the velocity and microrotation profiles. The values of Pr are chosen as 600

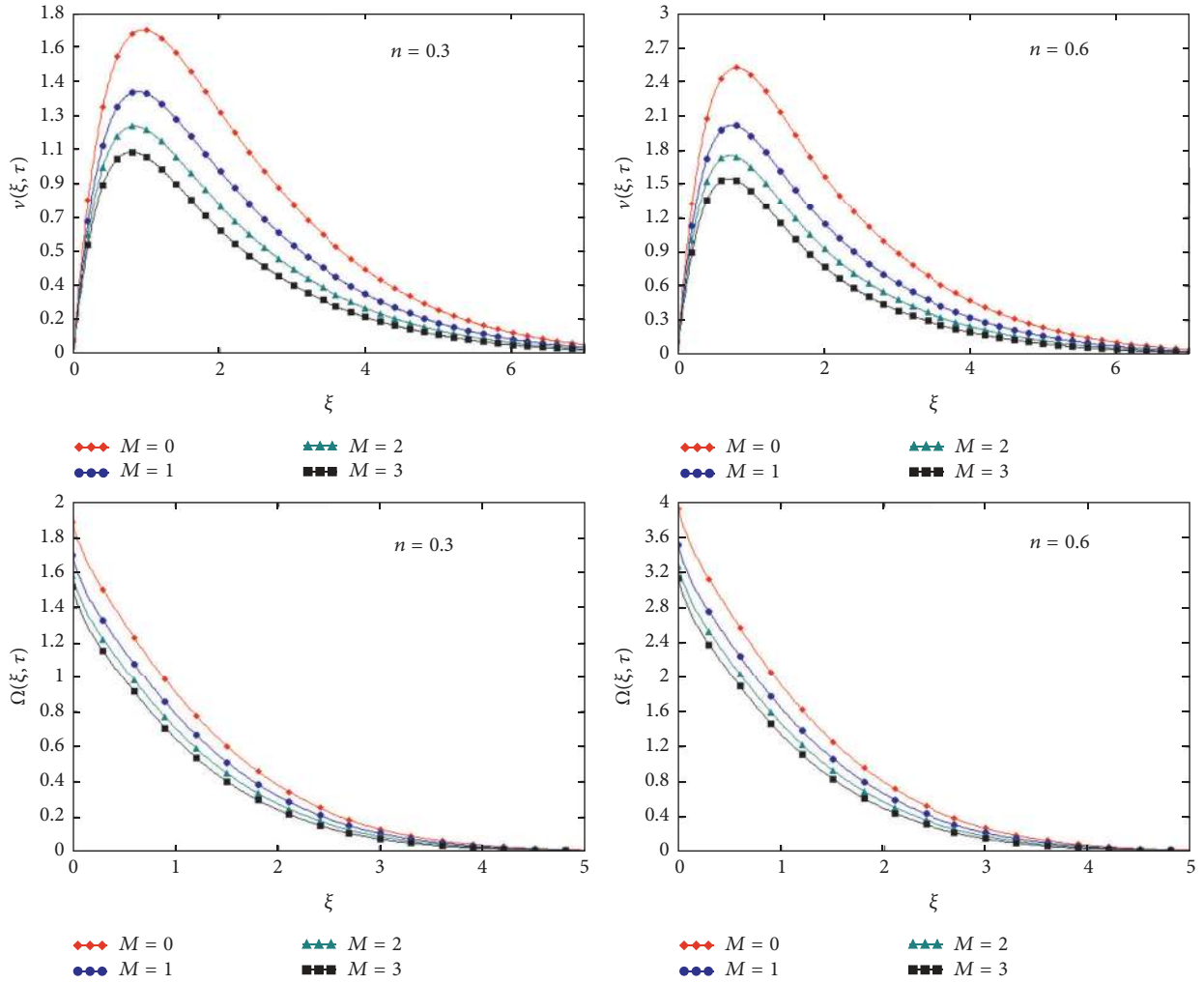

Figure 3: Variation in velocity and microrotation for different value of M and n.

(light oil) and 1000 (glycerol). Physically greater values of Pr decrease thermal conductivity and enhance the viscous forces. Consequently, the fluid velocity and the magnitude of microrotation decrease. The influence of thermal Grashof number Gr and mass Grashof number Gm on velocity and microrotation is depicted from Figures 8–11. Increasing values of both these parameters are responsible for the rise in buoyancy forces and reducing viscous forces which result in an increase in fluid velocity and magnitude of microrotation. Figures 12 and 13 are sketched to show the effect of spin gradient viscosity parameter η on the velocity and microrotation profiles. In the case of the velocity profile, greater values of η decrease fluid velocity. However, microrotation increases with increasing η. The effect of β on the velocity and the microrotation profiles is shown in Figures 14 and 15. A decreasing behavior is observed for increasing values of β in both cases. In these figures, the comparison of micropolar fluid velocity with Newtonian fluid velocity is also sketched. The velocity of the micropolar fluid is smaller as compared to Newtonian fluid. It is true due to the fact that the boundary layer thickness of micropolar fluid is greater than the boundary layer thickness of the Newtonian fluid.

Table 1: Variations in coefficients of skin friction and couple stress for different values of K, M, and R.

K	M	R	C_f	C_s
0.5	1	0.2	6.006	7.641
1	1	0.2	5.546	7.868
1.5	1	0.2	5.386	7.956
0.5	**2**	0.2	6.437	7.46
0.5	**3**	0.2	6.843	7.313
0.5	1	**0.4**	8.635	7.613
0.5	1	**0.6**	29.444	7.571

In Table 1, the effects of M, K, and R on the skin friction C_f and couple stress coefficient C_s are presented. It is observed that increasing values of K reduce C_f which as a result enhances the fluid velocity, while greater values of K give rise to C_s. The effects of different values of M on C_f are calculated. It is noted that C_f is the increasing function of M, which is quite opposite behavior of M to that of velocity as shown in Figures 2–15, whereas C_s decreases with the increase

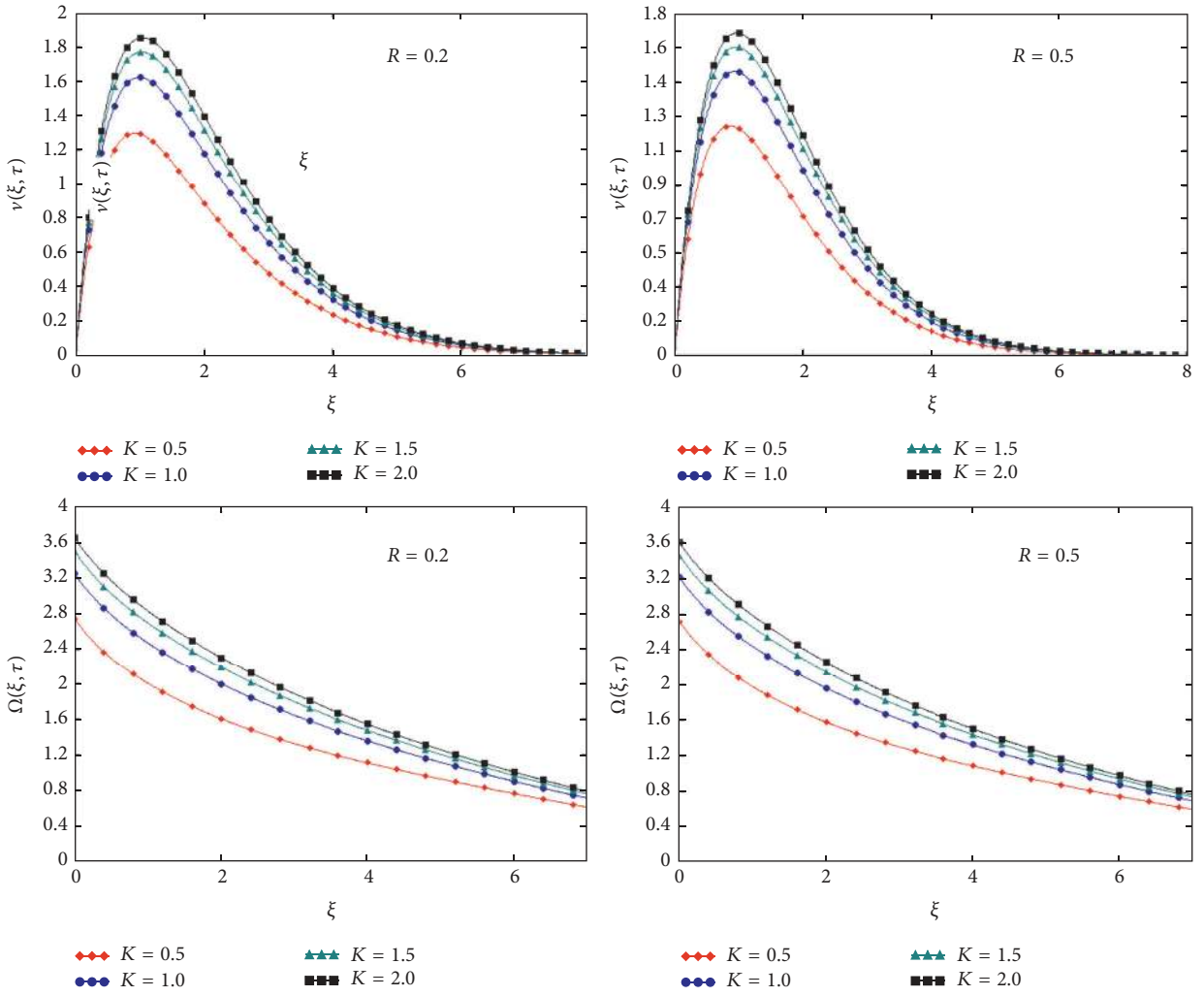

Figure 4: Variation in velocity and microrotation for different value of K and R.

in M. It is clear from the table that, for increasing values of R, C_f increases. This behavior of R is quite opposite to that of velocity. The effect of R on C_s is noticed opposite to that of C_f.

5. Conclusion

Unsteady MHD flow of micropolar fluid over an oscillating vertical plate embedded in a porous medium along with combined heat and mass transfer is studied. Exact solutions are obtained using the Laplace transform technique. The effects of different parameters on velocity and microrotation are discussed. The following main points are concluded from this work:

(i) An increase in M reduces the fluid velocity and magnitude of microrotation.

(ii) Velocity and magnitude of microrotation are directly related to K that causes fall in drag forces.

(iii) Velocity and magnitude of microrotation decrease as Pr is increased.

(iv) For large values of β, the velocity decreases.

(v) The skin friction increases with increase in M.

Appendix

One has

$$A_0 = \frac{1}{2} - nG_1 i\omega R_{14},$$

$$A_1 = \frac{1}{2} - nG_1 i\omega R_{13},$$

$$A_2 = \lambda_0 + \lambda_1,$$

$$A_3 = \lambda_0 - nG_1 a_{11} R_9,$$

$$A_4 = \lambda_1 - nG_1 a_{12} R_{10},$$

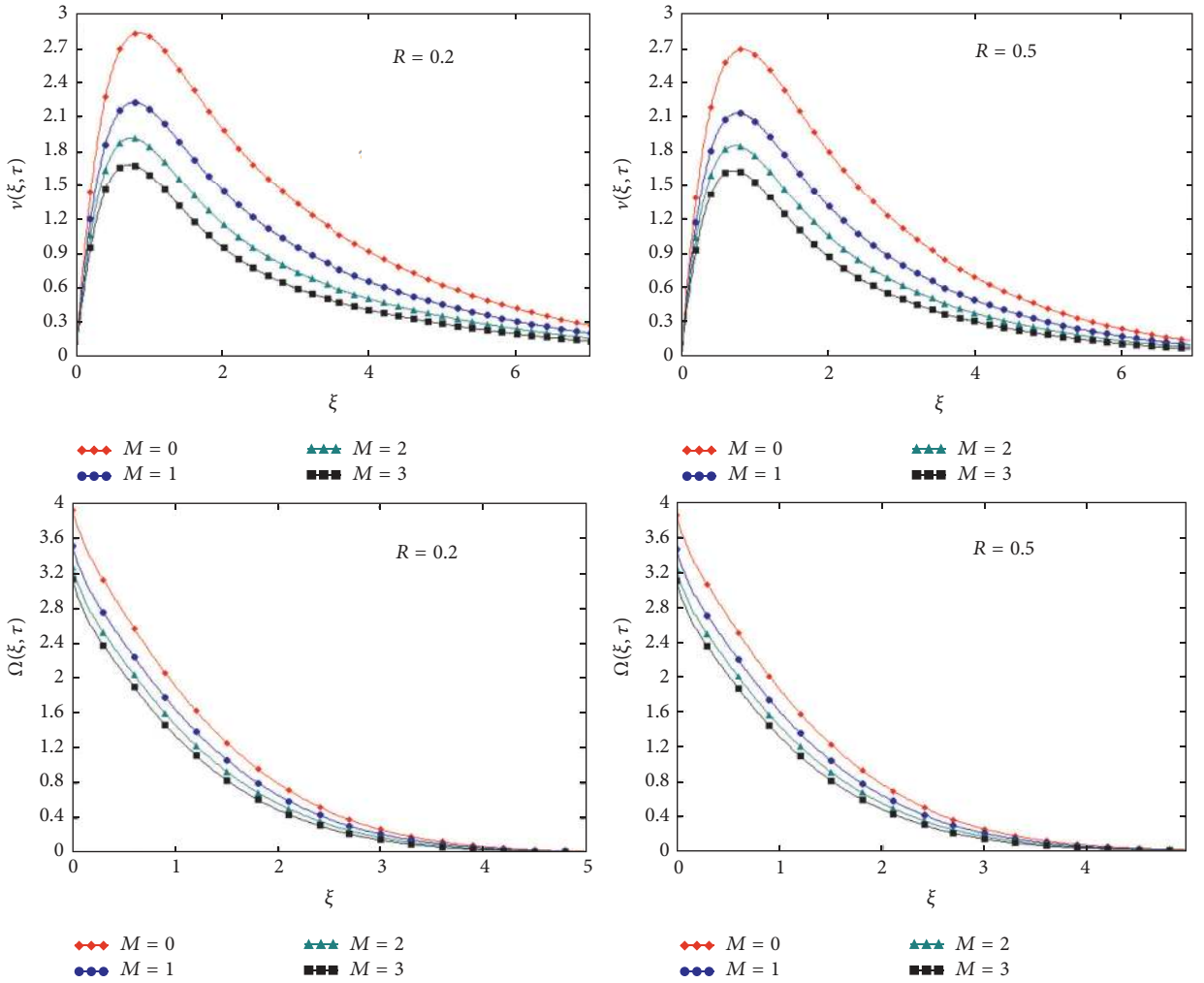

Figure 5: Variation in velocity and microrotation for different value of M and R.

$$A_5 = nG_1\delta_1 R_{11},$$

$$A_6 = nG_1\delta_2 R_{12},$$

$$A_7 = nG_1\delta_3 A_2,$$

$$A_8 = nG_1 a_{11} R_9,$$

$$A_9 = nG_1 a_{12} R_{10},$$

$$A_{10} = i\omega nG_1 R_{13},$$

$$A_{11} = i\omega nG_1 R_{14},$$

$$A_{12} = nG_1 R_1\sqrt{\delta},$$

$$A_{13} = nG_1 A_1\sqrt{\delta},$$

$$A_{14} = nG_1 R_2\sqrt{\delta},$$

$$A_{15} = nG_1 R_3\sqrt{\delta},$$

$$A_{16} = nG_1 R_4\sqrt{\delta},$$

$$A_{17} = nG_1 R_5\sqrt{\delta},$$

$$A_{18} = nG_1 R_6\sqrt{\delta},$$

$$A_{19} = nG_1 R_7\sqrt{\delta},$$

$$R_1 = \frac{L_1}{\delta_3},$$

$$R_2 = \frac{L_2}{a_{11} - \delta_3},$$

$$R_3 = \frac{L_3}{a_{12} - \delta_3},$$

$$R_4 = \frac{L_4}{\delta_1 + \delta_3},$$

$$R_5 = \frac{L_5}{\delta_2 + \delta_3},$$

$$R_6 = \frac{L_6}{i\omega - \delta_3},$$

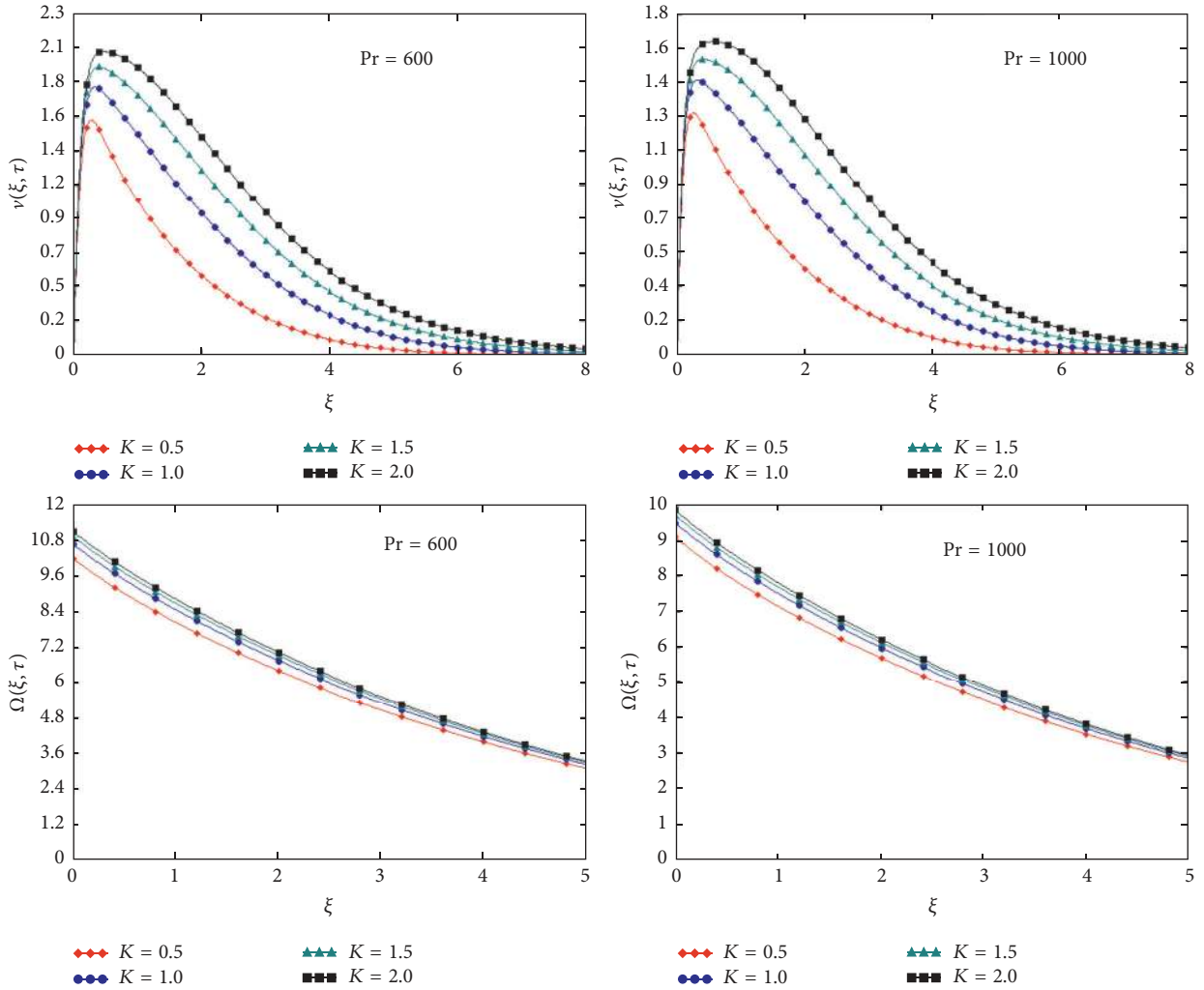

Figure 6: Variation in velocity and microrotation for different value of K and Pr.

$$R_7 = \frac{L_7}{i\omega + \delta_3},$$

$$R_8 = \frac{L_8}{\delta_3},$$

$$R_9 = \frac{a_{11}L_9}{a_{11} - \delta_3},$$

$$R_{10} = \frac{a_{12}L_{10}}{a_{12} - \delta_3},$$

$$R_{11} = \frac{L_{11}}{\delta_1 + \delta_3},$$

$$R_{12} = \frac{L_{12}}{\delta_2 + \delta_3},$$

$$R_{13} = \frac{L_{13}}{i\omega - \delta_3},$$

$$R_{14} = \frac{L_{14}}{i\omega + \delta_3},$$

$$\lambda_0 = \frac{G_2}{a_{11}},$$

$$\lambda_1 = \frac{G_3}{a_{12}},$$

$$A_1 = R_1 - R_2 - R_3 + R_4 + R_5 - R_6 + R_7,$$

$$A_2 = R_8 - R_9 - R_{10} + R_{11} + R_{12} - R_{13} + R_{14},$$

$$L_1 = -C_0 + C_1 + C_4 - \overline{C}_0 + \overline{C}_1 + \overline{C}_4,$$

$$L_2 = C_0 - C_2 - C_5 - \overline{H}_7 + \overline{H}_8 + H_9 - H_{10},$$

$$L_3 = \overline{C}_0 - \overline{C}_2 - \overline{C}_5 - \overline{H}_7 - \overline{H}_8 + \overline{H}_9 - \overline{H}_{10},$$

$$L_4 = -C_3 - \overline{C}_3 + H_7 + \overline{H}_7 - \overline{H}_9 - H_9 - l_3,$$

$$\boxed{L_5 = -C_6 - \overline{C}_6 - H_8 + H_{10} - \overline{H}_8 + \overline{H}_{10} + l_6}$$

$$L_6 = l_0 - l_1 - l_4,$$

$$L_7 = l_0 + l_2 + l_5,$$

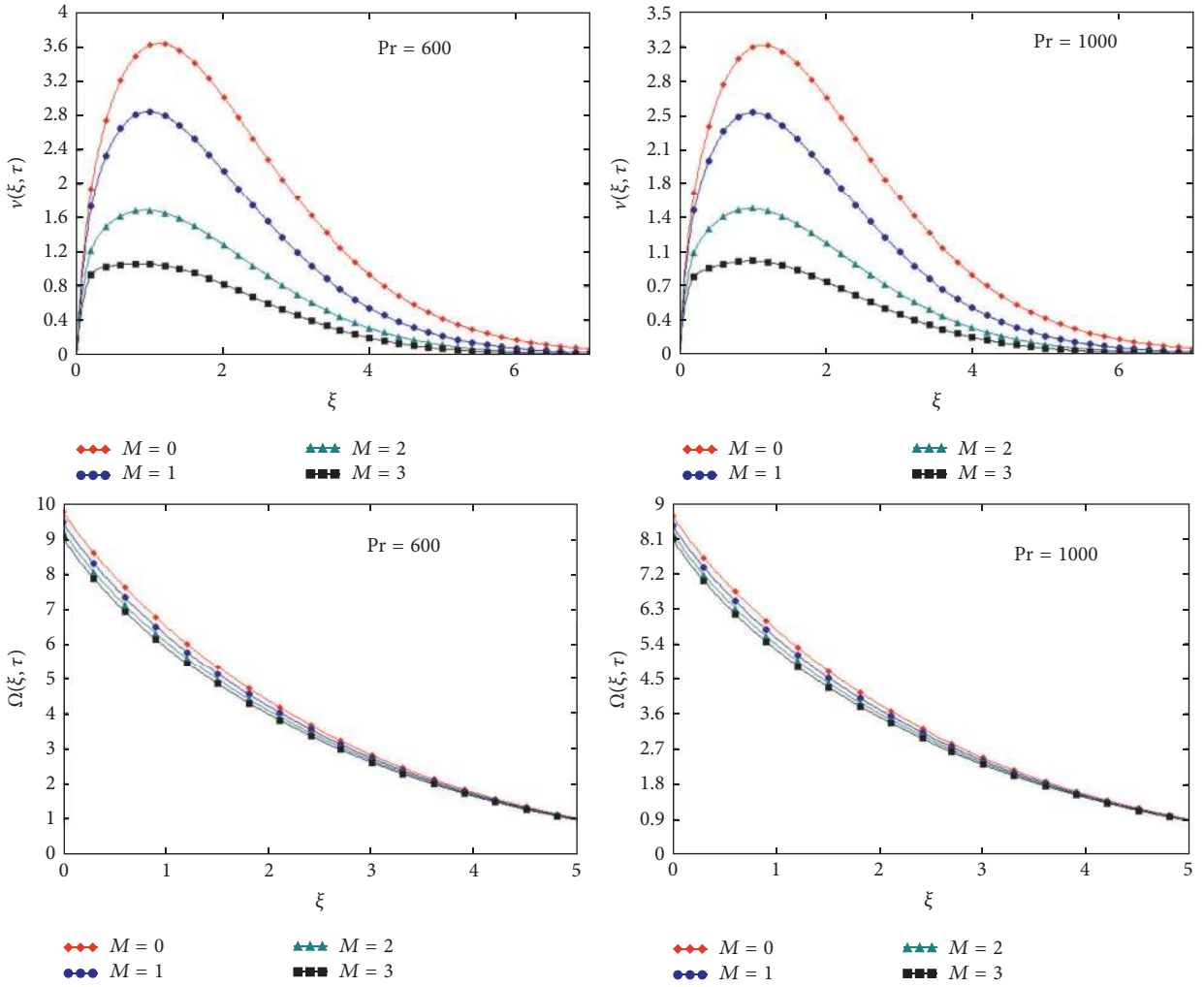

Figure 7: Variation in velocity and microrotation for different value of M and Pr.

$$L_8 = -C_7 + C_{11} + C_{14} - C_{17} - \overline{C}_7 + \overline{C}_{11} + \overline{C}_{14} - \overline{C}_{17} + H_0 - H_1 - H_4 + \overline{H}_0 - \overline{H}_1 - \overline{H}_4,$$

$$L_9 = C_8 - C_{12} - C_{15} + C_{18} - H_0 + H_2 + H_5,$$

$$L_{10} = \overline{C}_8 - \overline{C}_{12} - \overline{C}_{15} + \overline{C}_{18} - \overline{H}_0 + \overline{H}_2 + \overline{H}_5,$$

$$L_{11} = C_9 - C_{16} + \overline{C}_9 - \overline{C}_{16} + H_3 - \overline{H}_3 - l_9 - l_{15},$$

$$L_{12} = -C_{13} + C_{19} - \overline{C}_{13} + \overline{C}_{19} + H_6 - \overline{H}_6 + l_{12} - l_{18},$$

$$L_{13} = l_7 - l_{10} - l_{13} + l_{16},$$

$$L_{14} = -l_8 + l_{11} + l_{14} - l_{17},$$

$$l_0 = \frac{W_o}{2},$$

$$l_1 = \frac{W_1}{2(i\omega + \delta_1)},$$

$$l_2 = \frac{W_1}{2(i\omega - \delta_1)},$$

$$l_3 = \frac{W_1\delta_1}{2(\omega^2 - \delta_1^2)},$$

$$l_4 = \frac{W_2}{2(i\omega + \delta_2)},$$

$$l_5 = \frac{W_2}{2(i\omega - \delta_2)},$$

$$l_6 = \frac{W_1\delta_2}{2(\omega^2 - \delta_2^2)},$$

$$l_7 = \frac{\delta W_3(K_{\text{eff}} + i\omega)}{2i\omega(\delta_1 + i\omega)},$$

$$l_8 = \frac{\delta W_3(-K_{\text{eff}} + i\omega)}{2i\omega(-\delta_1 + i\omega)},$$

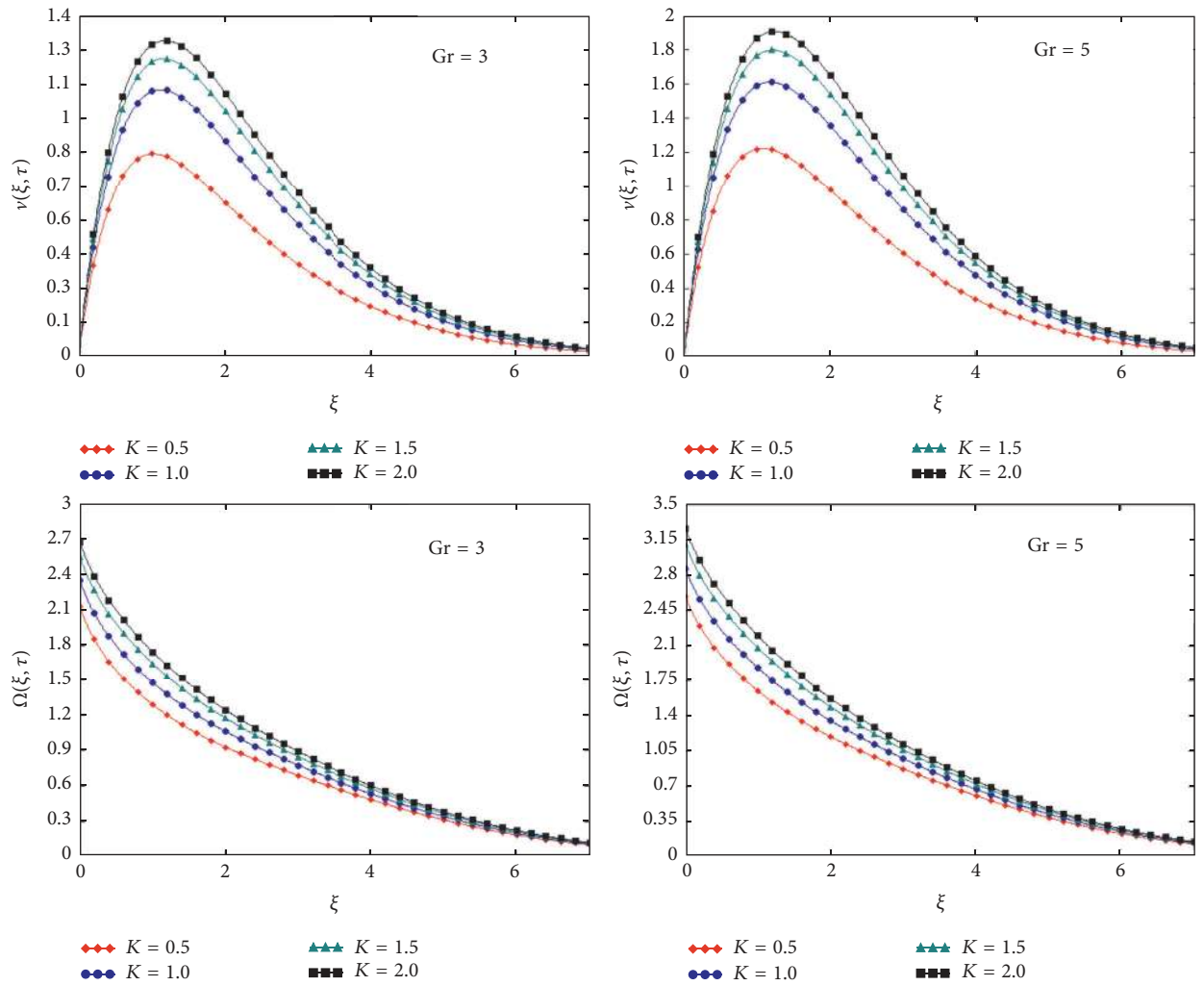

Figure 8: Variation in velocity and microrotation for different value of K and Gr.

$$l_9 = \frac{\delta W_3 \left(-K_{\text{eff}} + i\omega\right)}{2i\omega\left(\delta_1^2 + \omega^2\right)},$$

$$l_{10} = \frac{\delta W_3 \left(K_{\text{eff}} + i\omega\right)}{2i\omega\left(\delta_2 + i\omega\right)},$$

$$l_{11} = \frac{\delta W_3 \left(-K_{\text{eff}} + i\omega\right)}{2i\omega\left(-\delta_2 + i\omega\right)},$$

$$l_{12} = \frac{\delta W_3 \left(-K_{\text{eff}} + i\omega\right)}{2i\omega\left(\delta_2^2 + \omega^2\right)},$$

$$l_{13} = \frac{\delta W_4 \left(K_{\text{eff}} + i\omega\right)}{2i\omega\left(\delta_1 + i\omega\right)},$$

$$l_{14} = \frac{\delta W_4 \left(-K_{\text{eff}} + i\omega\right)}{2i\omega\left(-\delta_1 + i\omega\right)},$$

$$l_{15} = \frac{\delta W_4 \left(-K_{\text{eff}} + i\omega\right)}{2i\omega\left(\delta_1^2 + \omega^2\right)},$$

$$l_{16} = \frac{\delta W_4 \left(K_{\text{eff}} + i\omega\right)}{2i\omega\left(\delta_2 + i\omega\right)},$$

$$l_{17} = \frac{\delta W_4 \left(-K_{\text{eff}} + i\omega\right)}{2i\omega\left(-\delta_2 + i\omega\right)},$$

$$l_{18} = \frac{\delta W_4 \left(-K_{\text{eff}} + i\omega\right)}{2i\omega\left(\delta_2^2 + \omega^2\right)},$$

$$H_0 = \frac{a_9 g_1 W_0}{a_{11}},$$

$$H_1 = \frac{a_9 g_1 W_1}{a_{11}\delta_1},$$

$$H_2 = \frac{a_9 g_1 W_1}{a_{11}\left(\delta_1 + a_{11}\right)},$$

$$H_3 = \frac{a_9 g_1 W_1}{\delta_1\left(\delta_1 + a_{11}\right)},$$

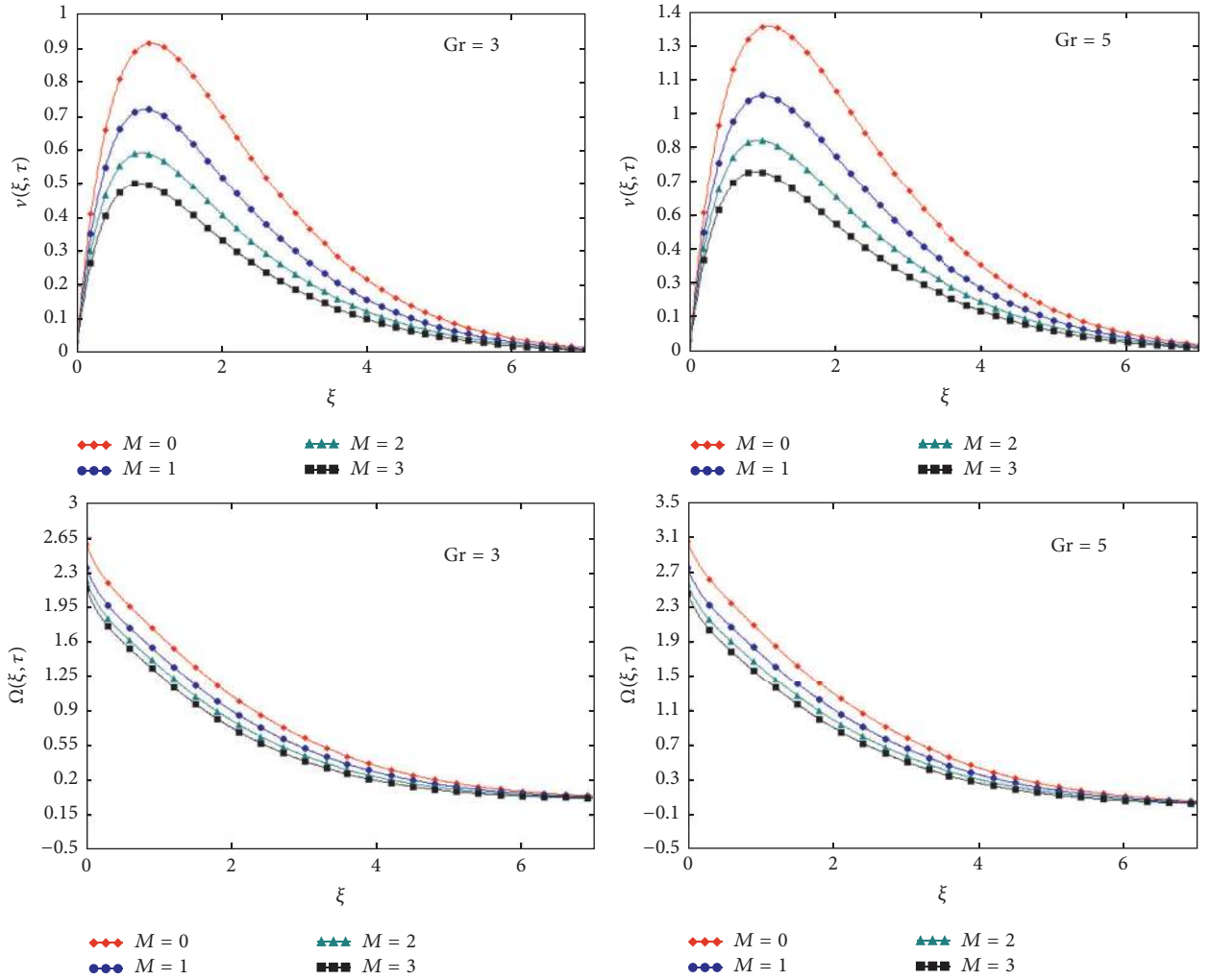

Figure 9: Variation in velocity and microrotation for different value of M and Gr.

$$H_4 = \frac{a_9 g_1 W_2}{a_{11}\delta_2},$$

$$H_5 = \frac{a_9 g_1 W_2}{a_{11}(\delta_2 + a_{11})},$$

$$H_6 = \frac{a_9 g_1 W_2}{\delta_2(\delta_2 + a_{11})},$$

$$H_7 = \frac{a_9 g_1 W_3}{\delta_1 + a_{11}},$$

$$H_8 = \frac{a_9 g_l W_3}{\delta_2 + a_{11}},$$

$$H_9 = \frac{a_9 g_1 W_4}{\delta_1 + a_{11}},$$

$$H_{10} = \frac{a_9 g_1 W4}{\delta_2 + a_{11}},$$

$$\overline{H}_0 = \frac{a_9 g_2 W_0}{a_{12}},$$

$$\overline{H}_1 = \frac{a_9 g_2 W_1}{a_{12}\delta_1},$$

$$\overline{H}_2 = \frac{a_9 g_2 W_1}{a_{12}(\delta_1 + a_{12})},$$

$$\overline{H}_3 = \frac{a_9 g_2 W_1}{\delta_1(\delta_1 + a_{12})},$$

$$\overline{H}_4 = \frac{a_9 g_2 W_2}{a_{12}\delta_2},$$

$$\overline{H}_5 = \frac{a_9 g_2 W_2}{a_{12}(\delta_2 + a_{12})},$$

$$\overline{H}_6 = \frac{a_9 g_2 W_2}{\delta_2(\delta_2 + a_{12})},$$

$$\overline{H}_7 = \frac{a_9 g_2 W_3}{\delta_1 + a_{12}},$$

$$\overline{H}_8 = \frac{a_9 g_2 W_3}{\delta_2 + a_{12}},$$

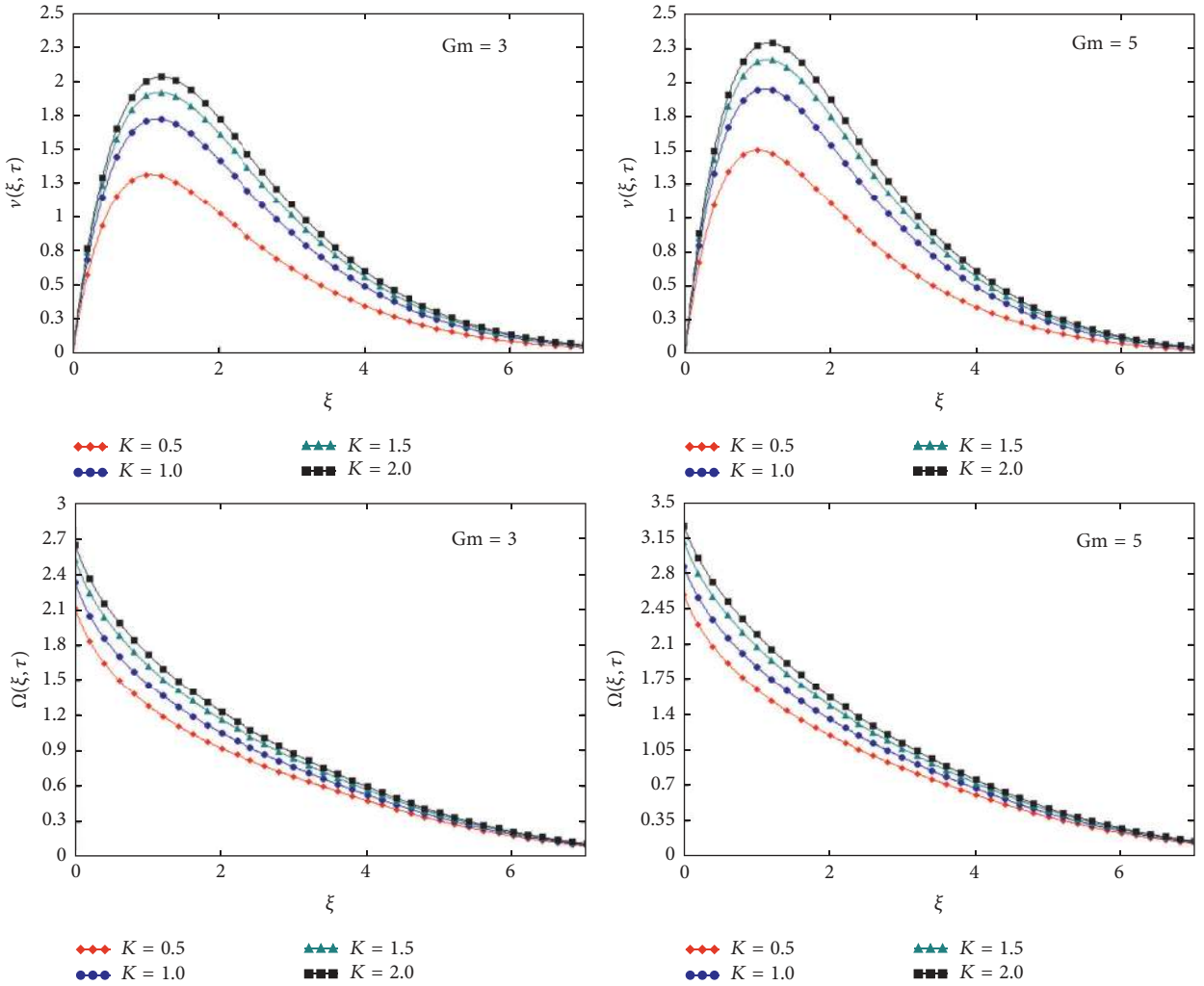

Figure 10: Variation in velocity and microrotation for different value of K and Gm.

$$\overline{H}_9 = \frac{a_9 g_2 W_4}{\delta_1 + a_{12}},$$

$$\overline{H}_{10} = \frac{a_9 g_2 W_4}{\delta_2 + a_{12}},$$

$$C_0 = \frac{g_1 W_1}{a_{11}},$$

$$C_1 = \frac{g_1 W_1}{a_{11}\delta_1},$$

$$C_2 = \frac{g_1 W_1}{a_{11}(\delta_1 + a_{11})},$$

$$C_3 = \frac{g_1 W_1}{\delta_1(\delta_1 + a_{11})},$$

$$C_4 = \frac{g_1 W_2}{a_{11}\delta_2},$$

$$C_5 = \frac{g_1 W_2}{a_{11}(\delta_2 + a_{11})},$$

$$C_6 = \frac{g_1 W_2}{\delta_2(\delta_2 + a_{11})},$$

$$C_7 = \frac{\delta g_1 K_{\text{eff}} W_3}{a_{11}\delta_1},$$

$$C_8 = \frac{\delta g_1 W_3 (a_{11} + K_{\text{eff}})}{a_{11}(\delta_1 + a_{11})},$$

$$C_9 = \frac{\delta g_1 W_3 (K_{\text{eff}} - \delta_1)}{\delta_1(\delta_1 + a_{11})},$$

$$C_{11} = \frac{\delta g_1 K_{\text{eff}} W_3}{a_{11}\delta_2},$$

$$C_{12} = \frac{\delta g_1 W_3 (a_{11} + K_{\text{eff}})}{a_{11}(\delta_2 + a_{11})},$$

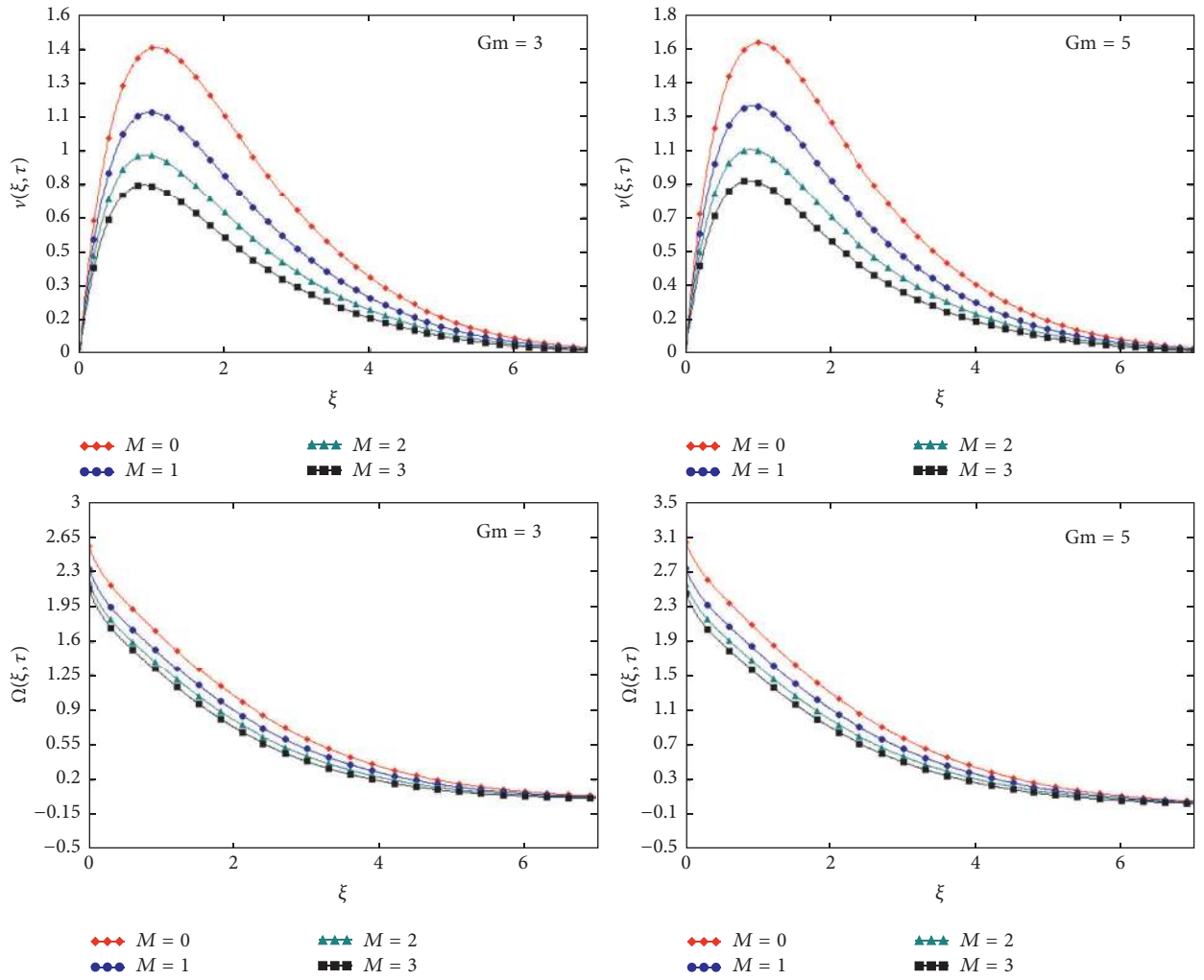

Figure 11: Variation in velocity and microrotation for different value of M and Gr.

$$C_{13} = \frac{\delta g_1 W_3 (K_{\text{eff}} - \delta_2)}{\delta_2 (\delta_2 + a_{11})},$$

$$C_{14} = \frac{\delta g_1 K_{\text{eff}} W_4}{a_{11} \delta_1},$$

$$C_{15} = \frac{\delta g_1 W_4 (a_{11} + K_{\text{eff}})}{a_{11} (\delta_1 + a_{11})},$$

$$C_{16} = \frac{\delta g_1 W_4 (K_{\text{eff}} - \delta_1)}{\delta_1 (\delta_1 + a_{11})},$$

$$C_{17} = \frac{\delta g_1 K_{\text{eff}} W_4}{a_{11} \delta_2},$$

$$C_{18} = \frac{\delta g_1 W_4 (a_{11} + K_{\text{eff}})}{a_{11} (\delta_2 + a_{11})},$$

$$C_{19} = \frac{\delta g_1 W_4 (K_{\text{eff}} - \delta_2)}{\delta_2 (\delta_2 + a_{11})},$$

$$\overline{C}_0 = \frac{g_2 W_1}{a_{12}},$$

$$\overline{C}_1 = \frac{g_2 W_1}{a_{12} \delta_1},$$

$$\overline{C}_2 = \frac{g_2 W_1}{a_{12} (\delta_1 + a_{12})},$$

$$\overline{C}_3 = \frac{g_2 W_1}{\delta_1 (\delta_1 + a_{12})},$$

$$\overline{C}_4 = \frac{g_2 W_2}{a_{12} \delta_2},$$

$$\overline{C}_5 = \frac{g_2 W_2}{a_{12} (\delta_2 + a_{12})},$$

$$\overline{C}_6 = \frac{g_2 W_2}{\delta_2 (\delta_2 + a_{12})},$$

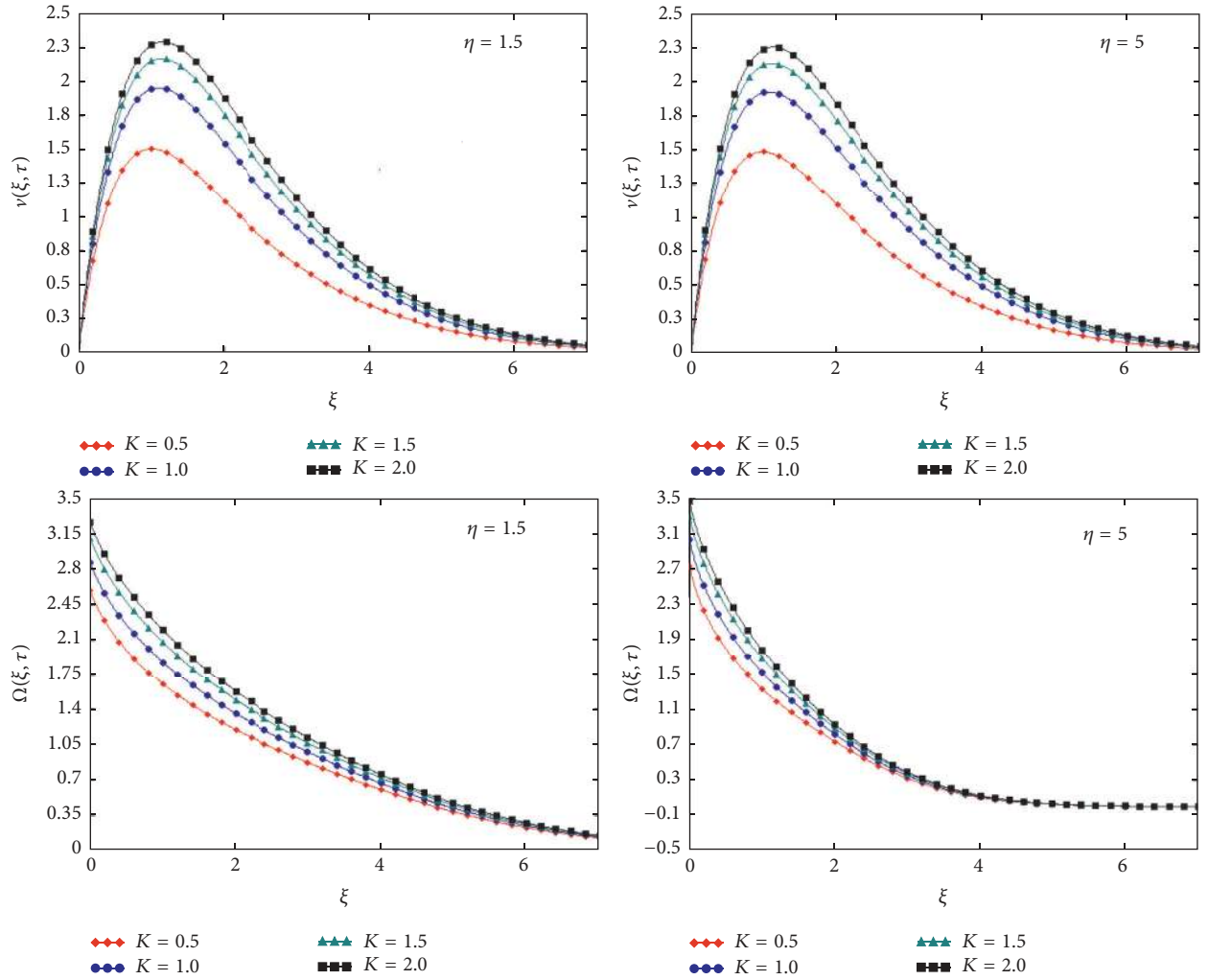

Figure 12: Variation in velocity and microrotation for different value of K and η.

$$\overline{C}_7 = \frac{\delta g_2 K_{\text{eff}} W_3}{a_{12}\delta_1},$$

$$\overline{C}_8 = \frac{\delta g_2 W_3 (a_{12} + K_{\text{eff}})}{a_{12}(\delta_1 + a_{12})},$$

$$\overline{C}_9 = \frac{\delta g_2 W_3 (K_{\text{eff}} - \delta_1)}{\delta_1(\delta_1 + a_{12})},$$

$$\overline{C}_{11} = \frac{\delta g_2 K_{\text{eff}} W_3}{a_{12}\delta_2},$$

$$\overline{C}_{12} = \frac{\delta g_2 W_3 (a_{12} + K_{\text{eff}})}{a_{12}(\delta_2 + a_{12})},$$

$$\overline{C}_{13} = \frac{\delta g_2 W_3 (K_{\text{eff}} - \delta_2)}{\delta_2(\delta_2 + a_{12})},$$

$$\overline{C}_{14} = \frac{\delta g_2 K_{\text{eff}} W_4}{a_{12}\delta_1},$$

$$\overline{C}_{15} = \frac{\delta g_2 W_4 (a_{12} + K_{\text{eff}})}{a_{12}(\delta_1 + a_{12})},$$

$$\overline{C}_{16} = \frac{\delta g_2 W_4 (K_{\text{eff}} - \delta_1)}{\delta_1(\delta_1 + a_{12})},$$

$$\overline{C}_{17} = \frac{\delta g_2 K_{\text{eff}} W_4}{a_{12}\delta_2},$$

$$\overline{C}_{18} = \frac{\delta g_2 W_4 (a_{12} + K_{\text{eff}})}{a_{12}(\delta_2 + a_{12})},$$

$$\overline{C}_{19} = \frac{\delta g_2 W_4 (K_{\text{eff}} - \delta_2)}{\delta_2(\delta_2 + a_{12})},$$

$$W_0 = 1 - d_8,$$

$$W_1 = \frac{d_9\delta_1 - d_8\delta_1^2}{\delta_1 - \delta_2},$$

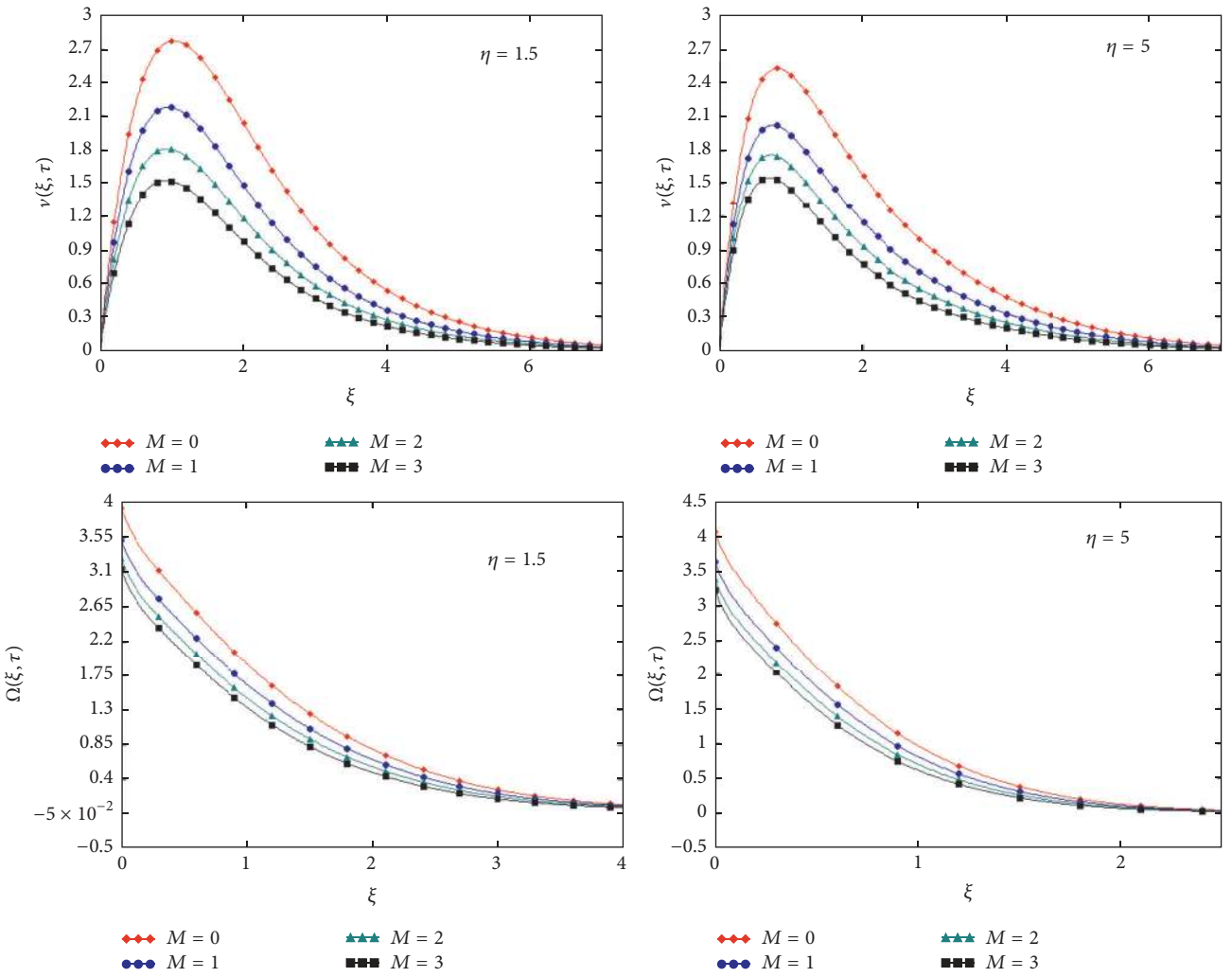

Figure 13: Variation in velocity and microrotation for different value of M and η.

$$W_2 = \frac{d_9\delta_2 - d_8\delta_2^2}{\delta_1 - \delta_2},$$

$$W_3 = \frac{d_6}{\delta_1 - \delta_2},$$

$$W_4 = \frac{d_7}{\delta_1 - \delta_2},$$

$$d_1 = a_2 - a_8,$$

$$d_2 = d_1^2 + a_1^2\delta n^2,$$

$$d_3 = 2a_3d_1 + a_1^2\delta K_{\text{eff}} n^2,$$

$$d_4 = a_2d_1 - d_1^2 + a_1^2\delta K_{\text{eff}} n^2,$$

$$d_5 = -a_2a_3 + a_3d_1 + a_1^2\delta K_{\text{eff}} n^2,$$

$$d_6 = \frac{a_1a_3n}{d_2},$$

$$d_7 = \frac{a_1a_2n}{d_2},$$

$$d_8 = \frac{d_4}{d_2},$$

$$d_9 = \frac{d_5}{d_2},$$

$$\delta_1 = \frac{m_2}{2} + \frac{\sqrt{m_2^2 - 4m_1a_3}}{2},$$

$$\delta_2 = \frac{m_2}{2} - \frac{\sqrt{m_2^2 - 4m_1a_3}}{2},$$

$$\delta_3 = \frac{a_3}{a_2},$$

$$G_1 = \frac{a_1}{a_2},$$

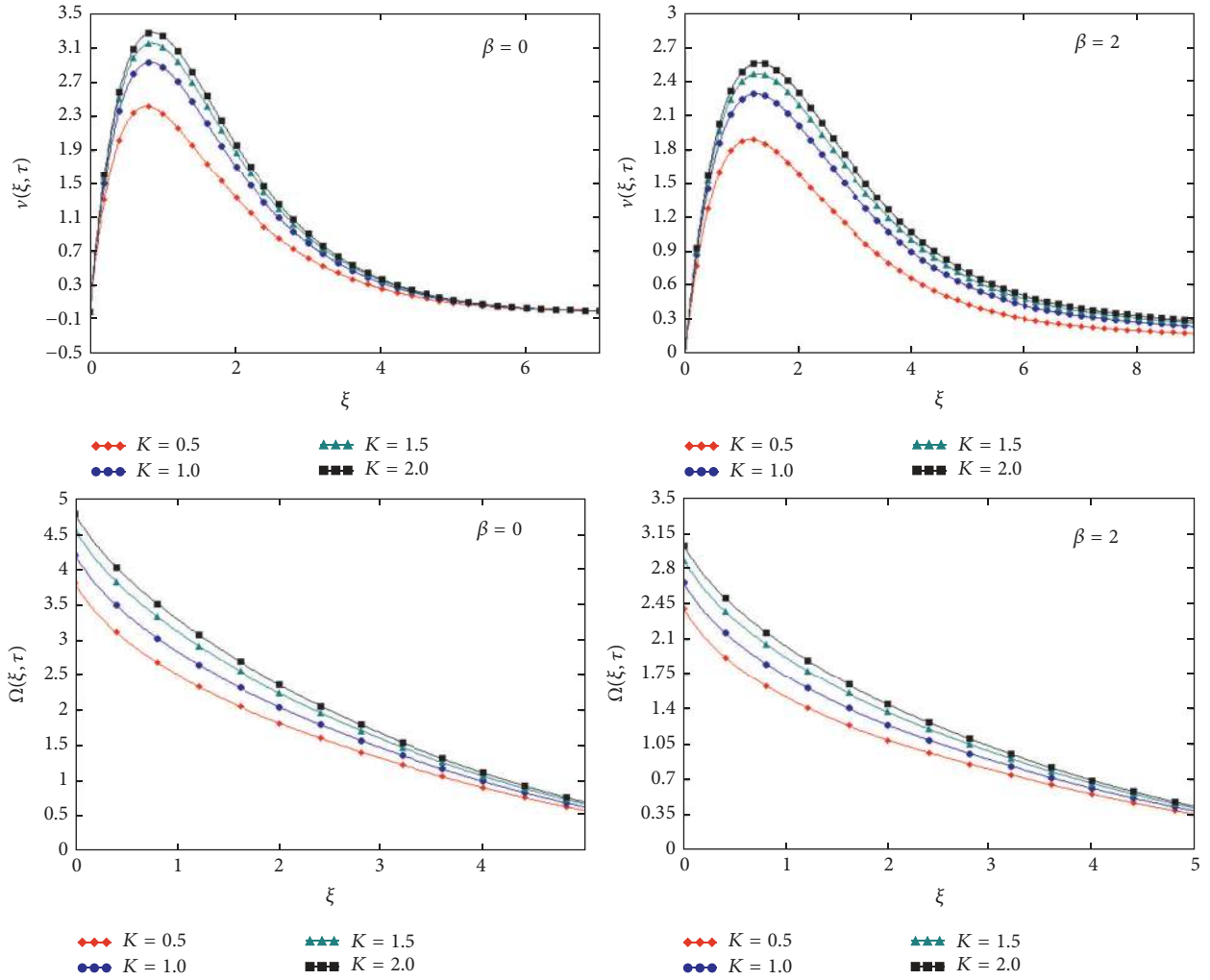

Figure 14: Variation in velocity and microrotation for different value of K and β.

$$G_2 = \mathrm{Gr}\frac{\delta}{a_5},$$

$$G_3 = \mathrm{Gm}\frac{\delta}{a_7},$$

$$m_1 = \frac{a_3}{d_2},$$

$$m_2 = \frac{d_3}{d_2},$$

$$m_3 = \frac{d_1}{d_2},$$

$$g_1 = \frac{a_4}{a_5},$$

$$g_2 = \frac{a_6}{a_7},$$

$$a_{11} = \frac{a_3}{a_5},$$

$$a_{12} = \frac{a_3}{a_7},$$

$$a_1 = \beta\delta\sqrt{\eta},$$

$$a_2 = \eta - \delta,$$

$$a_3 = K_{\mathrm{eff}}\delta,$$

$$a_4 = \delta\mathrm{Gr},$$

$$a_5 = \mathrm{Pr}_{\mathrm{eff}} - \delta,$$

$$a_6 = \delta\mathrm{Gm},$$

$$a_7 = \mathrm{Sc} - \delta,$$

$$a_8 = n\eta\beta\delta,$$

$$a_9 = n\sqrt{\mathrm{Pr}_{\mathrm{eff}}},$$

$$a_{10} = n\sqrt{\mathrm{Sc}},$$

$$\delta = \frac{1}{1+\beta}. \tag{A.1}$$

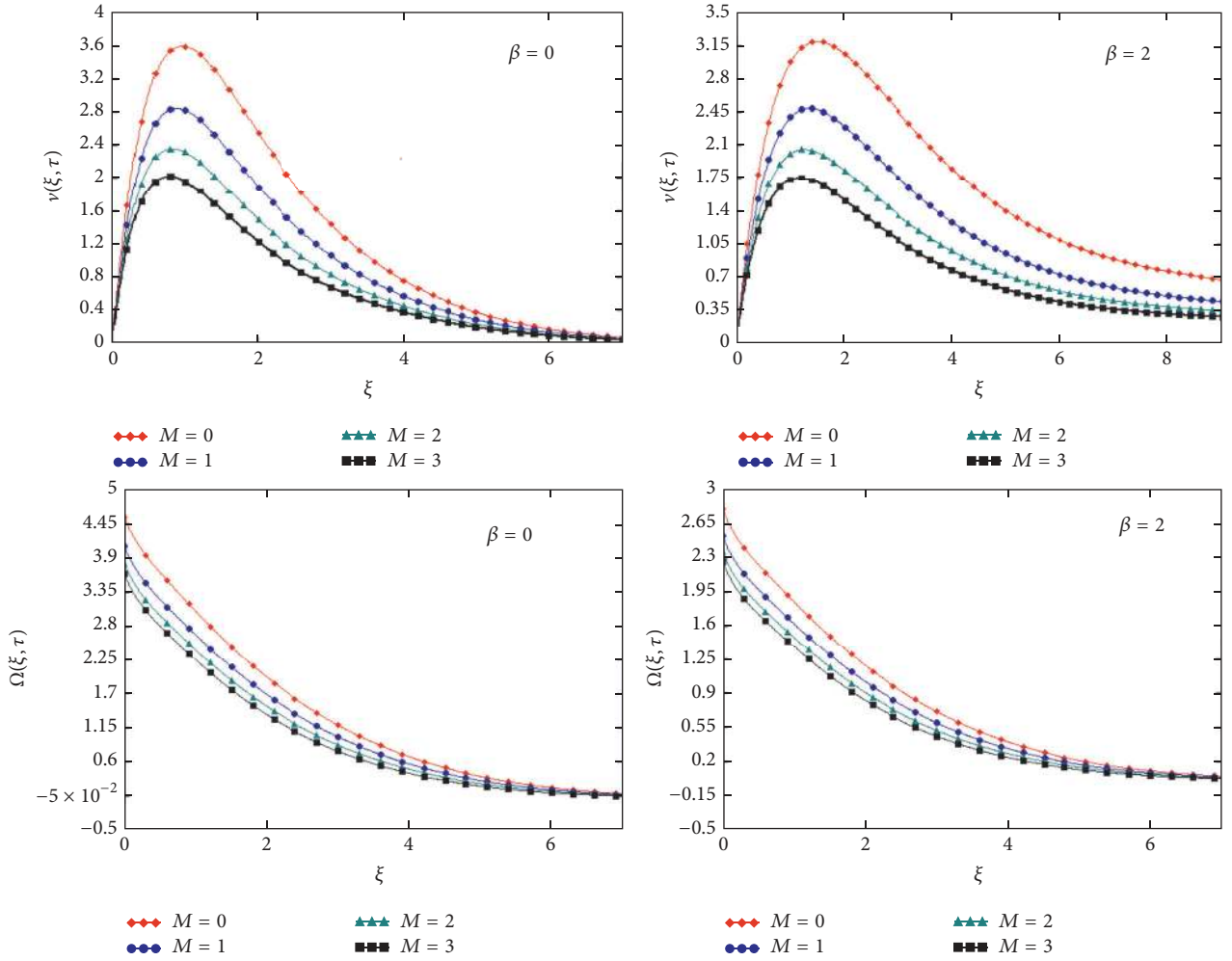

Figure 15: Variation in velocity and microrotation for different value of M and β.

Competing Interests

The authors declare that there are no competing interests regarding the publication of this paper.

References

[1] T. Hayat, C. Fetecau, and M. Sajid, "Analytic solution for MHD transient rotating flow of a second grade fluid in a porous space," *Nonlinear Analysis: Real World Applications*, vol. 9, no. 4, pp. 1619–1627, 2008.

[2] A. Khan, I. Khan, F. Ali, S. Ulhaq, and S. Shafie, "Effects of wall shear stress on unsteady MHD conjugate flow in a porous medium with ramped wall temperature," *PLoS ONE*, vol. 9, no. 3, Article ID e90280, 2014.

[3] O. Prakash, D. Kumar, and Y. K. Dwivedi, "Effects of thermal diffusion and chemical reaction on MHD flow of dusty visco-elastic (Walter's liquid model-B) fluid," *Journal of Electromagnetic Analysis and Applications*, vol. 2, no. 10, pp. 581–587, 2010.

[4] N. Shahid, "A study of heat and mass transfer in a fractional MHD flow over an infinite oscillating plate," *SpringerPlus*, vol. 4, no. 1, article 640, 2015.

[5] C. S. K. Raju and N. Sandeep, "Heat and mass transfer in MHD non-Newtonian bio-convection flow over a rotating cone/plate with cross diffusion," *Journal of Molecular Liquids*, vol. 215, pp. 115–126, 2016.

[6] S. T. Mohyud-Din, Z. A. Zaidi, U. Khan, and N. Ahmed, "On heat and mass transfer analysis for the flow of a nanofluid between rotating parallel plates," *Aerospace Science and Technology*, vol. 46, pp. 514–522, 2015.

[7] D. Pal and S. Chatterjee, "Heat and mass transfer in MHD non-Darcian flow of a micropolar fluid over a stretching sheet embedded in a porous media with non-uniform heat source and thermal radiation," *Communications in Nonlinear Science and Numerical Simulation*, vol. 15, no. 7, pp. 1843–1857, 2010.

[8] M. A. Mansour, M. A. El-Hakiem, and S. M. El Kabeir, "Heat and mass transfer in magnetohydrodynamic flow of micropolar fluid on a circular cylinder with uniform heat and mass flux," *Journal of Magnetism and Magnetic Materials*, vol. 220, no. 2, pp. 259–270, 2000.

[9] S. Srinivas and M. Kothandapani, "The influence of heat and mass transfer on MHD peristaltic flow through a porous space with compliant walls," *Applied Mathematics and Computation*, vol. 213, no. 1, pp. 197–208, 2009.

[10] M. M. Rahman and M. A. Sattar, "Magnetohydrodynamic convective flow of a micropolar fluid past a continuously moving vertical porous plate in the presence of heat generation/absorption," *Journal of Heat Transfer*, vol. 128, no. 2, pp. 142–152, 2006.

[11] M. S. Alam, M. M. Rahman, and M. A. Sattar, "Effects of variable suction and thermophoresis on steady MHD combined free-forced convective heat and mass transfer flow over a semi-infinite permeable inclined plate in the presence of thermal radiation," *International Journal of Thermal Sciences*, vol. 47, no. 6, pp. 758–765, 2008.

[12] N. T. Eldabe and M. E. M. Ouaf, "Chebyshev finite difference method for heat and mass transfer in a hydromagnetic flow of a micropolar fluid past a stretching surface with Ohmic heating and viscous dissipation," *Applied Mathematics and Computation*, vol. 177, no. 2, pp. 561–571, 2006.

[13] A. A. Bakr, "Effects of chemical reaction on MHD free convection and mass transfer flow of a micropolar fluid with oscillatory plate velocity and constant heat source in a rotating frame of reference," *Communications in Nonlinear Science and Numerical Simulation*, vol. 16, no. 2, pp. 698–710, 2011.

[14] D. B. Ingham and I. Pop, *Transport Phenomena in Porous Media*, Elsevier, 1998.

[15] E. M. Abo-Eldahab and A. F. Ghonaim, "Radiation effect on heat transfer of a micropolar fluid through a porous medium," *Applied Mathematics and Computation*, vol. 169, no. 1, pp. 500–510, 2005.

[16] Y. J. Kim, "Heat and mass transfer in MHD micropolar flow over a vertical moving porous plate in a porous medium," *Transport in Porous Media*, vol. 56, no. 1, pp. 17–37, 2004.

[17] M. Modather, A. M. Rashad, and A. J. Chamkha, "An analytical study of MHD heat and mass transfer oscillatory flow of a micropolar fluid over a vertical permeable plate in a porous medium," *Turkish Journal of Engineering and Environmental Sciences*, vol. 33, no. 4, pp. 245–257, 2009.

[18] A. Khalid, I. Khan, A. Khan, and S. Shae, "Unsteady MHD free convection ow of Casson fluid past over an oscillating vertical plate embedded in a porous medium," *Engineering Science and Technology, an International Journal*, vol. 18, no. 3, pp. 309–317, 2015.

[19] S. Nadeem, R. U. Haq, N. S. Akbar, and Z. H. Khan, "MHD three-dimensional Casson fluid flow past a porous linearly stretching sheet," *Alexandria Engineering Journal*, vol. 52, no. 4, pp. 577–582, 2013.

[20] F. Ali, M. Norzieha, S. Sharidan, I. Khan, and T. Hayat, "New exact solutions of Stokes' second problem for an MHD second grade fluid in a porous space," *International Journal of Non-Linear Mechanics*, vol. 47, no. 5, pp. 521–525, 2012.

[21] T. Hayat, R. Sajjad, Z. Abbas, M. Sajid, and A. A. Hendi, "Radiation effects on MHD flow of Maxwell fluid in a channel with porous medium," *International Journal of Heat and Mass Transfer*, vol. 54, no. 4, pp. 854–862, 2011.

[22] A. Khalid, I. Khan, and S. Shafie, "Heat transfer in ferrofluid with cylindrical shape nanoparticles past a vertical plate with ramped wall temperature embedded in a porous medium," *Journal of Molecular Liquids*, vol. 221, pp. 1175–1183, 2016.

[23] A. M. Abd-Alla, S. M. Abo-Dahab, and R. D. Al-Simery, "Effect of rotation on peristaltic flow of a micropolar fluid through a porous medium with an external magnetic field," *Journal of Magnetism and Magnetic Materials*, vol. 348, pp. 33–43, 2013.

[24] A. Shakir, T. Gul, and S. Islam, "Analysis of MHD and thermally conducting unsteady thin lm flow in a porous medium," *Journal of Applied Environmental and Biological Sciences*, vol. 5, no. 1, 2015.

[25] E. M. Abo-Eldahab and M. A. El Aziz, "Flow and heat transfer in a micropolar fluid past a stretching surface embedded in a non-Darcian porous medium with uniform free stream," *Applied Mathematics and Computation*, vol. 162, no. 2, pp. 881–899, 2005.

[26] A. C. Eringen, "A unified theory of thermomechanical materials," *International Journal of Engineering Science*, vol. 4, no. 2, pp. 179–202, 1966.

[27] F. Ali, I. Khan, S. Shafie, and N. Musthapa, "Heat and mass transfer with free convection MHD flow past a vertical plate embedded in a porous medium," *Mathematical Problems in Engineering*, vol. 2013, Article ID 346281, 13 pages, 2013.

[28] R. Nazar, N. Amin, D. Filip, and I. Pop, "Stagnation point flow of a micropolar fluid towards a stretching sheet," *International Journal of Non-Linear Mechanics*, vol. 39, no. 7, pp. 1227–1235, 2004.

[29] S. Nadeem, M. Hussain, and M. Naz, "MHD stagnation flow of a micropolar fluid through a porous medium," *Meccanica*, vol. 45, no. 6, pp. 869–880, 2010.

[30] A. Raptis, "Flow of a micropolar fluid past a continuously moving plate by the presence of radiation," *International Journal of Heat and Mass Transfer*, vol. 41, no. 18, pp. 2865–2866, 1998.

[31] M. Qasim, I. Khan, and S. Shafie, "Heat transfer in a micropolar fluid over a stretching sheet with Newtonian heating," *PLoS ONE*, vol. 8, no. 4, Article ID e59393, 2013.

[32] I. Papautsky, J. Brazzle, T. Ameel, and A. B. Frazier, "Laminar fluid behavior in microchannels using micropolar fluid theory," *Sensors and Actuators, A: Physical*, vol. 73, no. 1-2, pp. 101–108, 1999.

[33] M. A. El-Hakiem, A. A. Mohammadein, S. M. M. El-Kabeir, and R. S. R. Gorla, "Joule heating effects on magnetohydrodynamic free convection flow of a micropolar fluid," *International Communications in Heat and Mass Transfer*, vol. 26, no. 2, pp. 219–227, 1999.

[34] K. Das, "Effect of chemical reaction and thermal radiation on heat and mass transfer flow of MHD micropolar fluid in a rotating frame of reference," *International Journal of Heat and Mass Transfer*, vol. 54, no. 15-16, pp. 3505–3513, 2011.

[35] P. M. Patil and P. S. Kulkarni, "Effects of chemical reaction on free convective flow of a polar fluid through a porous medium in the presence of internal heat generation," *International Journal of Thermal Sciences*, vol. 47, no. 8, pp. 1043–1054, 2008.

[36] A. Hussanan, M. Z. Salleh, I. Khan, and R. M. Tahar, "Heat and mass transfer in a micropolar fluid with Newtonian heating: an exact analysis," *Neural Computing and Applications*, pp. 1–9, 2016.

[37] A. Khalid, I. Khan, A. Khan, and S. Shafie, "Conjugate transfer of heat and mass in unsteady flow of a micropolar fluid with wall couple stress," *AIP Advances*, vol. 5, no. 12, Article ID 127125, 2015.